iScience

CellPress
OPEN ACCESS

Article

NanoLuc reporters identify *COL4A5* nonsense mutations susceptible to drug-induced stop codon readthrough

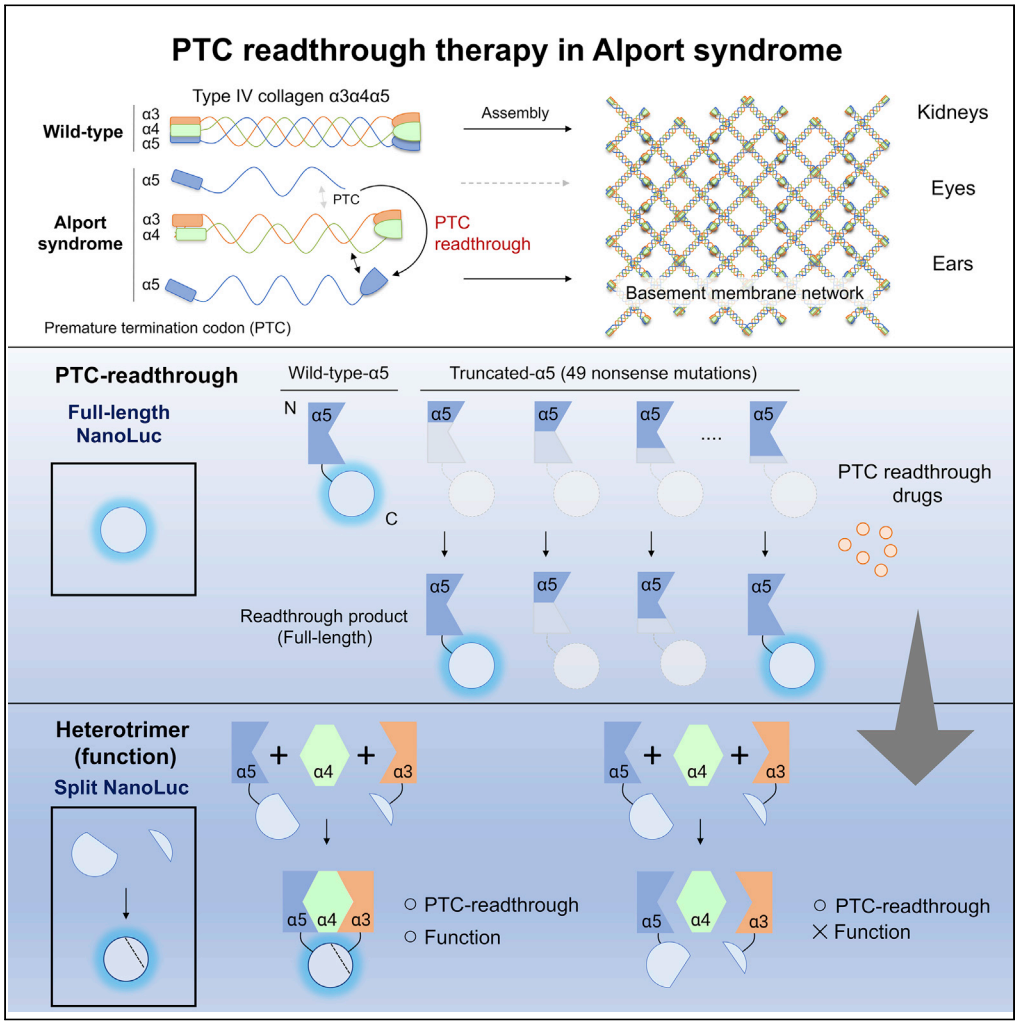

Kohei Omachi, Hirofumi Kai, Michel Roberge, Jeffrey H. Miner

minerj@wustl.edu

Highlights

NanoLuc fusion constructs identified *COL4A5* mutants susceptible to PTC readthrough

Readthrough enhancer and "designer" compounds promoted PTC readthrough

Split-NanoLuc fusion constructs identified functional missense readthrough products

Cultured *Col4a5* nonsense mutant mouse kidney cells were susceptible to readthrough

Omachi et al., iScience *25*, 103891
March 18, 2022
https://doi.org/10.1016/j.isci.2022.103891

iScience

CellPress
OPEN ACCESS

Article

NanoLuc reporters identify *COL4A5* nonsense mutations susceptible to drug-induced stop codon readthrough

Kohei Omachi,[1] Hirofumi Kai,[2] Michel Roberge,[3] and Jeffrey H. Miner[1,4,*]

SUMMARY

Alport syndrome, a disease of kidney, ear, and eye, is caused by pathogenic variants in the *COL4A3*, *COL4A4*, or *COL4A5* genes encoding collagen α3α4α5(IV) of basement membranes. Collagen IV chains that are truncated due to nonsense variants/premature termination codons (PTCs) cannot assemble into heterotrimers or incorporate into basement membranes. To investigate the feasibility of PTC readthrough therapy for Alport syndrome, we utilized two NanoLuc reporters in transfected cells: full-length for monitoring translation, and a split version for assessing readthrough product function. Full-length assays of 49 *COL4A5* nonsense variants identified eleven as susceptible to PTC readthrough using various readthrough drugs. In split-NanoLuc assays, the predicted missense α5(IV) readthrough products of five nonsense mutations could heterotrimerize with α3(IV) and α4(IV). Readthrough was also observed in kidney cells from an engineered *Col4a5* PTC mouse model. These results suggest that readthrough therapy is a feasible approach for a fraction of patients with Alport syndrome.

INTRODUCTION

Alport syndrome is a hereditary kidney glomerular disease with eye and inner ear defects characterized by glomerular basement membrane (GBM) abnormalities leading to progressive glomerulosclerosis and kidney failure (Hudson et al., 2003). Pathogenic variants in either the *COL4A3* (Morrison et al., 1991a, 1991b), *COL4A4* (Mochizuki et al., 1994) or *COL4A5* (Barker et al., 1990) genes encoding the type IV collagen α3, α4, and α5 chains, respectively, cause Alport syndrome. All three chains are necessary to form a functional type IV collagen α3α4α5 network. The chains assemble inside cells into α3α4α5 heterotrimers (protomers), which are secreted into the extracellular space (Gunwar et al., 1998), where they polymerize to build a basement membrane with other components such as laminins, nidogen, and heparan sulfate proteoglycans (Miner, 2011).

The lack or reduction of type IV collagen α3α4α5 in Alport syndrome eventually leads to GBM abnormalities including thinning, thickening, and splitting. Current standard-of-care therapy uses renin-angiotensin system inhibitors such as angiotensin-converting enzyme inhibitors or angiotensin II receptor blockers. Though they delay progression to kidney failure, they do not cure Alport syndrome (Gross et al., 2003, 2020; Yamamura et al., 2020b). In contrast, development of methods to fix the pathogenic GBM abnormalities compositional, structural, and functional could cure Alport syndrome or overcome the limitations of current treatments.

One of the potential barriers to the treatment of Alport syndrome using a GBM repair approach is the requirement that the abnormal GBM composed of collagen IV α1α1α2 be able to incorporate α3α4α5. Genetic rescue experiments in a *Col4a3*-null Alport syndrome mouse model has shown that postnatal induction of COL4A3 production in podocytes, the glomerular cells that normally synthesize the collagen IV α3α4α5 network, enables α3α4α5 trimer synthesis, secretion, and incorporation into the Alport GBM, which attenuates loss of kidney function (Lin et al., 2014). This study shows that restoration of the normal type IV collagen α3α4α5 network in the Alport GBM is a feasible approach toward a cure.

In the present study, we focused on chemical-induced restoration of COL4A5 expression in *COL4A5* nonsense variant types of Alport syndrome. Nonsense variants resulting in premature termination codons

[1]Division of Nephrology, Washington University School of Medicine, 4523 Clayton Avenue, St. Louis, MO 63110, USA

[2]Department of Molecular Medicine, Graduate School of Pharmaceutical Sciences, Kumamoto University, 5-1 Oe-honmachi, Chuo-ku, Kumamoto 862-0973, Japan

[3]Department of Biochemistry and Molecular Biology, University of British Columbia, Vancouver, BC V6T 1Z3, Canada

[4]Lead contact

*Correspondence: minerj@wustl.edu

https://doi.org/10.1016/j.isci.2022.103891

(PTCs) account for about 6% of Alport syndrome cases (Savige et al., 2016). Type IV collagen chains have a C-terminal NC1 domain that is essential for assembly of heterotrimers inside cells and for network formation in the GBM. Truncated α3, α4, α5 chains without an intact NC1 domain due to PTCs cannot form trimers or polymerize in the GBM (Sundaramoorthy et al., 2002). Therefore, achieving full-length protein expression is a potential therapy for Alport syndrome due to nonsense variants.

Small molecule-based PTC readthrough therapy has been well studied in other genetic diseases such as cystic fibrosis (Crawford et al., 2021; Du et al., 2006), Duchenne muscular dystrophy (Crawford et al., 2020; Kayali et al., 2012), and inherited skin disorders (Lincoln et al., 2018; Woodley et al., 2017). G418, an aminoglycoside class antibiotic, is the most studied drug that induces PTC readthrough. Aminoglycosides bind to prokaryotic ribosomes and inhibit protein synthesis in Gram-negative bacteria. In addition to their affinity for prokaryotic ribosomes, aminoglycosides are known to bind to eukaryotic ribosomes and induce PTC readthrough of nonsense variants by enabling near-cognate aminoacyl-tRNAs to recognize PTCs (Roy et al., 2015). Since the discovery of aminoglycoside-induced PTC readthrough, it has been shown that PTC readthrough can be induced by various aminoglycosides (Du et al., 2006; Friesen et al., 2018; Shulman et al., 2014). Although aminoglycoside-mediated PTC readthrough has the advantages of being well studied and highly efficient, high doses can cause nephrotoxicity and ototoxicity. To overcome these limitations, structurally designed aminoglycosides with reduced nephrotoxicity and ototoxicity that maintain readthrough activity have been developed (Shulman et al., 2014; Xue et al., 2014). In addition, non-aminoglycoside PTC readthrough compounds have been identified by high-throughput library screening (Du et al., 2009; Kayali et al., 2012), and some have been chemically modified to improve activity (Hamada et al., 2019; Taguchi et al., 2012, 2017). In addition, several compounds have been found to enhance the activity of PTC readthrough compounds, allowing the use of reduced doses of aminoglycosides and thus reduced toxicity (Baradaran-Heravi et al., 2016; Ferguson et al., 2019).

With these technological advances, PTC readthrough-based therapy has become a realistic option. However, whether nonsense readthrough therapy is applicable to Alport syndrome is unexplored. Here, we tested the feasibility of PTC readthrough therapy for X-linked Alport syndrome by generating a NanoLuc-based translation reporter system to evaluate which *COL4A5* nonsense variants are susceptible to readthrough therapy. Forty-nine nonsense variants reported in patients with Alport syndrome were tested, and 11 of them were highly sensitive to aminoglycoside-mediated PTC readthrough. Moreover, we found that designer aminoglycoside and non-aminoglycoside PTC readthrough drugs with reduced nephrotoxicity and ototoxicity induced synthesis of full-length PTC readthrough-sensitive variants. Also, PTC readthrough enhancer compounds potentiated aminoglycoside-mediated PTC readthrough. These results contribute important basic knowledge regarding the feasibility of PTC readthrough therapy in Alport syndrome and suggest that a fraction of patients should benefit from it.

RESULTS

Development of a NanoLuc-based COL4A5 translation reporter system

The efficacy of aminoglycoside-induced PTC readthrough varies greatly from variant to variant (Lincoln et al., 2018). At least, 76 *COL4A5* nonsense variants have been reported in patients with X-linked Alport syndrome, accounting for 6% of the known variants (Savige et al., 2016). Therefore, determining which nonsense variants are susceptible to PTC readthrough is a crucial first step toward clinical application. To evaluate the sensitivity of *COL4A5* nonsense variants to PTC readthrough in a high-throughput system, we generated a COL4A5-NanoLuc reporter plasmid by in-frame fusion of NanoLuc to the COOH-terminus of COL4A5 (Figure 1A). Introduction of a PTC into the COL4A5-NanoLuc cDNA leads to synthesis of truncated protein without the COOH-terminal NanoLuc, so luminescence is not produced. In this reporter system, it is assumed that a small molecule compound such as an aminoglycoside will promote PTC readthrough, leading to synthesis of a full-length protein and production of luminescence.

First, we introduced a pathogenic nonsense variant, R1563X, into the COL4A5-NanoLuc cDNA to see if we could detect PTC readthrough in the presence of G418, which is known to have high readthrough activity and is considered the gold standard PTC readthrough drug *in vitro*. G418 increased luminescence in HEK293 cells expressing COL4A5-R1563X-NanoLuc to a level that was 20%–30% of that of WT (Figure 1B). Moreover, to show that the PTC readthrough was not artifactually related to the presence of the NanoLuc RNA sequence in the transcript, we investigated whether G418 could induce PTC readthrough of COL4A5-R1563X mRNA, using COL4A5-R1563X-ΔNanoLuc (Figure 1C). Immunoblot analysis showed G418 induced

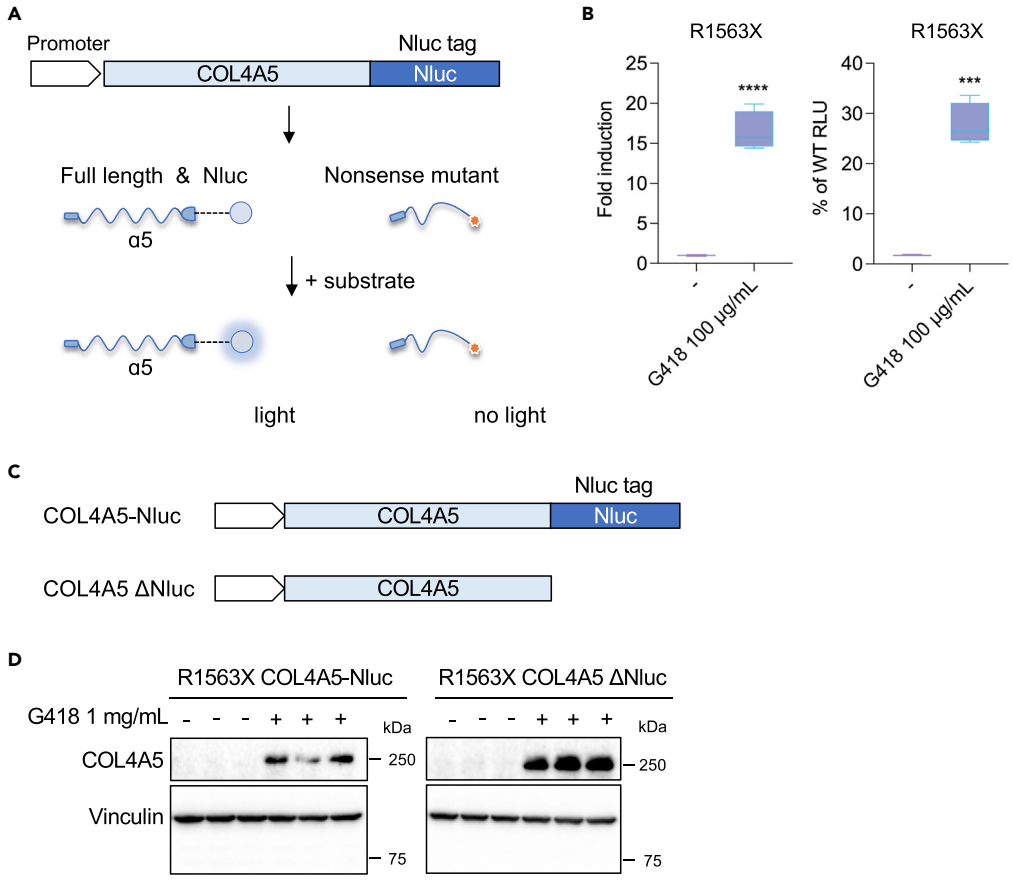

Figure 1. Development of a luciferase-based screening platform for testing PTC readthrough of *COL4A5* nonsense variants

(A) Schematic representation of the NanoLuc (Nluc) luciferase-based COL4A5 PTC readthrough reporter construct. Nluc was fused in-frame to the 3' end of the COL4A5 cDNA. Translation of full-length COL4A5 produces a fused functional Nluc that generates luminescence, but truncation of COL4A5 translation due to a PTC results in no luminescence.

(B) Luminescence was measured in cell lysates from HEK293 cells transfected with CMV-COL4A5-WT- and R1563X-NanoLuc plasmids and HSV-TK-Luc2 (firefly luciferase) for normalization. G418 treatment induced PTC readthrough. The box extends from the 25th to 75th percentiles. Data are represented as mean ± SEM. Statistical analysis was performed using Student's *t* test (n = 4). ***, $p < 0.005$; ****, $p < 0.001$ vs. non-treated.

(C) Schematics of NanoLuc-tagged (Nluc) and non-tagged (ΔNluc) COL4A5 expression constructs.

(D) Immunoblots of intracellular-Nluc-tagged or non-tagged COL4A5 products in HEK293 cells treated with G418 for 24 h. Full-length COL4A5 was detected by COL4A5 NC1 domain antibody (H52), and anti-Vinculin was used as loading control. G418 induced PTC readthrough of COL4A5-R1563X in both NanoLuc-tagged and non-tagged COL4A5-expressing cells. RLU, relative light units

PTC readthrough in HEK293 cells expressing either COL4A5-R1563X-NanoLuc or COL4A5-R1563X ΔNanoLuc (Figure 1D). These results show that the COL4A5-NanoLuc reporter cDNA was sensitive and quantitative enough for monitoring translation of full-length COL4A5 protein in a multi-well plate format.

Screening for PTC readthrough-susceptible *COL4A5* nonsense variants

To screen *COL4A5* nonsense variants reported in patients with X-linked Alport syndrome for susceptibility to PTC readthrough, we introduced 49 pathogenic variants individually into the COL4A5-NanoLuc cDNA reporter by site-directed mutagenesis. Nonsense variants in the collagenous domain that originally encoded Gly were excluded, because if the PTC readthrough product is not Gly, the Gly substitution will likely impair the function of the PTC readthrough product. Aminoglycoside-induced PTC variants are known to be influenced by the type of PTC (UGA > UAG > UAA) (Wangen and Green, 2020). Therefore, we selected all three types of nonsense variants for evaluation. Nonsense variant COL4A5-NanoLuc plasmids were

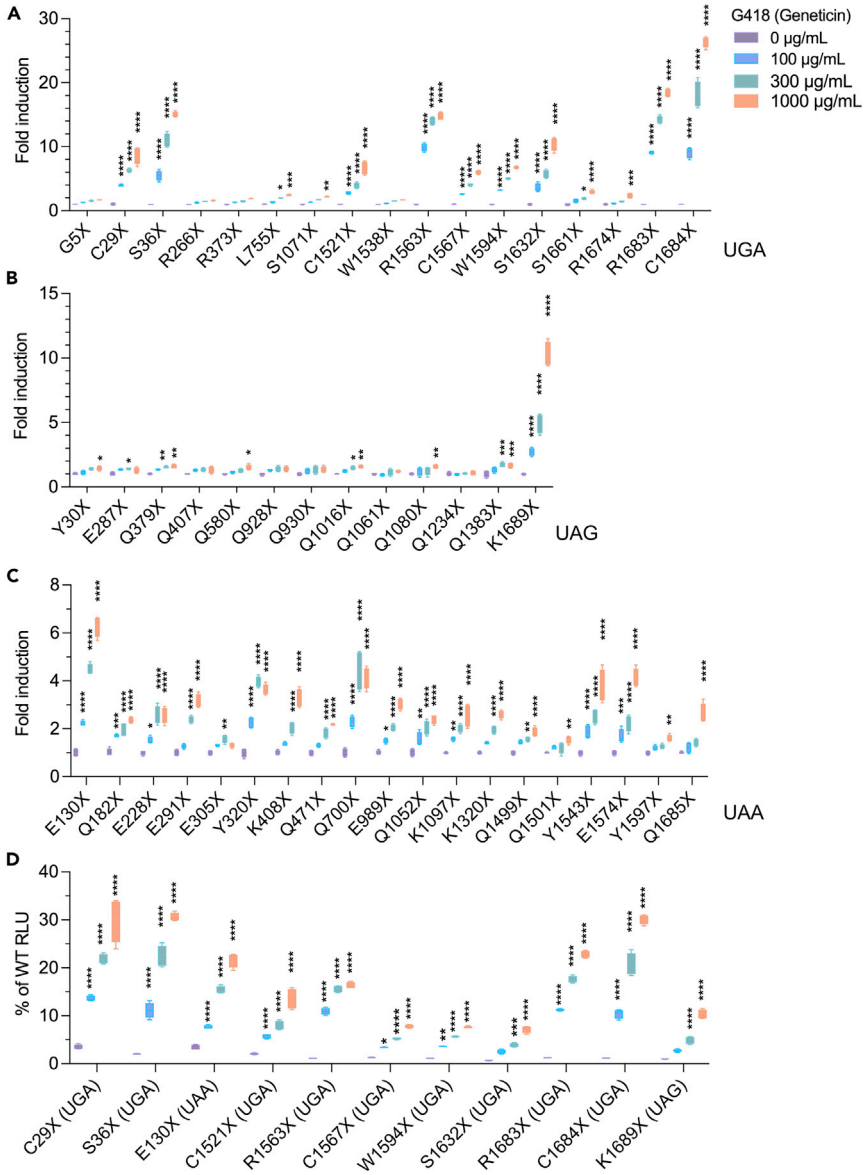

Figure 2. Identification of *COL4A5* variants susceptible to G418-induced PTC readthrough

(A–C) Luminescence was measured in cell lysates from HEK293 cells co-transfected with either CMV-NanoLuc-fused COL4A5-WT or the indicated nonsense variants and HSV-TK-Luc2 (firefly) for normalization. Cells expressing one UGA (A), UAG (B), or UAA (C) COL4A5 nonsense variant cDNA were treated with G418 at the indicated concentrations for 24 h, and luminescence was measured. G418 induced readthrough of some but not all PTCs. The box extends from the 25th to 75th percentiles. Data are represented as mean ± SEM.

(D) Readthrough efficiency of eleven readthrough-susceptible mutants was compared to WT. The box extends from the 25th to 75th percentiles. Data are represented as mean ± SEM. Statistical analysis was performed using two-way ANOVA with Tukey's multiple comparisons test (n = 4). *, $p < 0.05$; **, $p < 0.01$; ***, $p < 0.005$; ****, $p < 0.001$ vs. no treatment. RLU, relative light units

individually transfected into HEK293 cells, and the cells were treated for 24 h with different concentrations of G418. G418 induced significant PTC readthrough of 40 of the 49 nonsense variants (Figures 2A–2C). Many of them were statistically significant, but some did not have high PTC readthrough rates. Of the types of variants that responded to G418, UGA PTCs showed the highest readthrough rates, which agrees with previous studies. 11 of 49 *COL4A5* nonsense variants (*C29X, S36X, E130X, C1521X, R1563X, C1567X, W1594X, S1632X, R1683X, C1684X,* and *K1689X*) showed more than 5-fold induction of PTC readthrough.

The amount of luminescence produced from these G418-susceptible variants ranged from 10%–30% of the WT level (Figure 2D).

Gentamicin, an aminoglycoside approved for clinical use, induces PTC readthrough in G418-susceptible mutants

Although G418 is one of the most potent readthrough inducers, it is toxic and cannot be used clinically. Gentamicin is a clinically approved aminoglycoside class antibiotic. Therefore, we investigated whether gentamicin induced PTC readthrough of the G418-susceptible mutants. COL4A5-NanoLuc reporter cDNAs with introduced nonsense variants (*C29X, S36X, E130X, C1521X, R1563X, C1567X, W1594X, S1632X, R1683X, C1684X,* and *K1689X*) were transfected into HEK293 cells, and the extent of PTC readthrough induction by gentamicin treatment was quantified by measuring luminescence. Gentamicin significantly induced PTC readthrough of G418 susceptible variants except for *COL4A5-K1689X* (Figure 3A). The amount of full-length protein produced with gentamicin-induced readthrough peaked at 5%–10% of WT for most variants, which was 2–3 times less effective than G418 (Figure 3B). To further investigate PTC readthrough in different cell types, we examined 6 variants highly responsive to PTC readthrough using HeLa, mouse podocyte, and COS-7 cell lines. As in the experiments with HEK293 cells, wild-type and various variant plasmids were transfected into each cell line, and G418- and gentamicin-induced PTC readthrough were evaluated. Similar to HEK293 cells, both G418 and gentamicin induced PTC readthrough in the other cell types (Figures 3C and 3D).

The efficacy of aminoglycoside-mediated PTC readthrough is dose- and treatment time-dependent

To investigate whether aminoglycoside-induced PTC readthrough is treatment time-dependent, we performed long-term treatment experiments using low doses of aminoglycosides on cells expressing *COL4A5-R1563X* and *-R1683X* variants, which were highly responsive to G418 and gentamicin. For long-term treatment, we generated stable COL4A5-R1563X- and COL4A5-R1683X-NanoLuc cDNA-expressing cells by lentivirus transduction. The degree of PTC readthrough was increased with low-dose G418 treatment in a time-dependent manner (Figures 4A and 4B). The low concentrations of G418 (10 and 30 μg/mL) slightly increased readthrough, and the moderate concentration (100 μg/mL) dramatically increased full-length protein synthesis, depending on treatment time. The longer treatment with low concentrations of gentamicin (30 and 100 μg/mL) did not increase the efficacy of PTC readthrough, but readthrough was increased at the moderate (300 μg/mL) and high (1000 μg/mL) concentrations (Figures 4C and 4D).

Designer aminoglycoside and non-aminoglycoside readthrough drugs induce PTC readthrough in the highly susceptible variant *COL4A5-R1563X*

The potential for successful PTC readthrough therapy with aminoglycosides is dependent on their degrees of activity, nephrotoxicity, and ototoxicity (Forge and Schacht, 2000). Aminoglycoside toxicity is attributed to a structural site different from that responsible for PTC readthrough activity (Matt et al., 2012; Shulman et al., 2014). Therefore, chemical modification has been used to reduce the toxicity of aminoglycosides, with the aim of reducing toxicity while maintaining readthrough activity. Several aminoglycoside derivatives have been developed and are called designer aminoglycosides (Bidou et al., 2017). The use of PTC readthrough compounds with non-aminoglycoside structures is also a strategy to reduce toxicity. We tested a set of next-generation PTC readthrough drugs for efficacy at promoting readthrough of *COL4A5-R1563X*, a G418-susceptible mutant (Figure 2A). HEK293 cells expressing the COL4A5-R1563X-NanoLuc cDNA were treated with several PTC readthrough drugs for 24 h (Figure 5). Whereas G418 exhibited the highest readthrough activity (Figure 5A), ELX-02, the negamycin analog CDX008, RTC13, and 2,6-diaminopurine (DAP) significantly induced PTC readthrough dose dependently, but RTC14 and PTC124 did not (Figures 5B–5F and S1A). ELX-02 and DAP showed the highest PTC readthrough activity among them (Figures 5B and 5F). These results suggest that ELX-02, a designer aminoglycoside, and DAP, a purine derivative, have PTC readthrough activity for G418-sensitive variants such as R1563X, but they are expected to exhibit reduced toxicity.

Designer aminoglycoside and non-aminoglycoside PTC-RT drugs are ineffective for the non-G418-susceptible variant *COL4A5-G5X*

In addition to the G418-susceptible *COL4A5-R1563X* variant, we also tested whether any next generation PTC readthrough drugs induced PTC readthrough for the G418 non-susceptible *COL4A5-G5X* variant

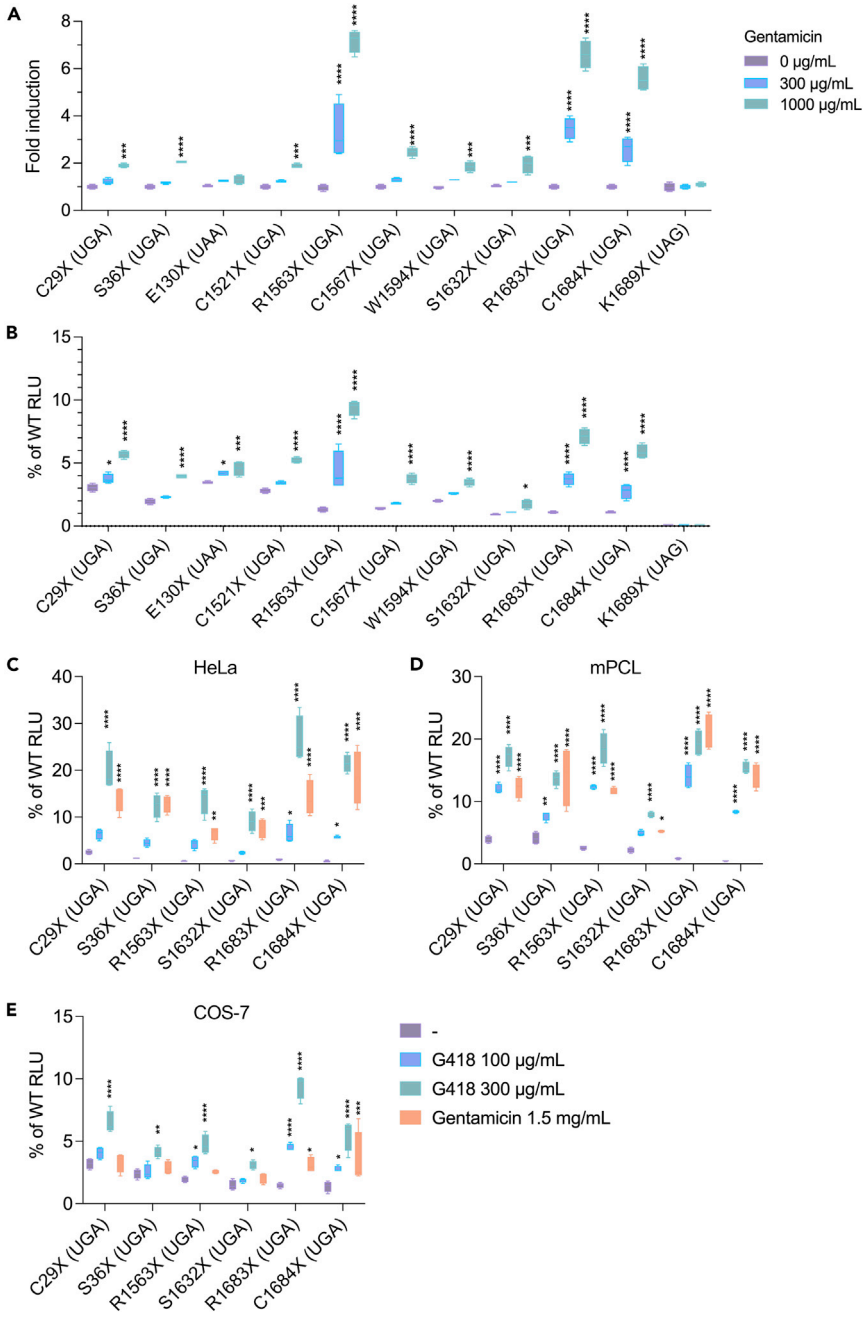

Figure 3. Gentamicin induces PTC readthrough of G418-susceptible *COL4A5* variants

(A) Luminescence was measured in cell lysates from HEK293 cells co-transfected with either CMV-NanoLuc-fused COL4A5-WT or the indicated nonsense variants and HSV-TK-Luc2 (firefly) for normalization. COL4A5-NanoLuc expressing cells were treated with gentamicin (as indicated) for 24 h, and luminescence was measured. The box extends from the 25th to 75th percentiles. Data are represented as mean ± SEM.

(B) Readthrough efficiency of eleven susceptible mutants was compared to WT.

(C–E) Luminescence was measured in cell lysates from HeLa cells (C), mouse Podocyte cell line (mPCL) (D), and COS-7 cells (E) co-transfected as in (A). COL4A5-NanoLuc-expressing cells were treated with gentamicin (as indicated) for 24 h, and luminescence was measured. Readthrough efficiency of six susceptible mutants was compared to WT. The box extends from the 25th to 75th percentiles. Data are represented as mean ± SEM. Statistical analysis was performed using two-way ANOVA with Tukey's multiple comparisons test (n = 4). *, $p < 0.05$; ***, $p < 0.005$; ****, $p < 0.001$. vs. no treatment. RLU, relative light units

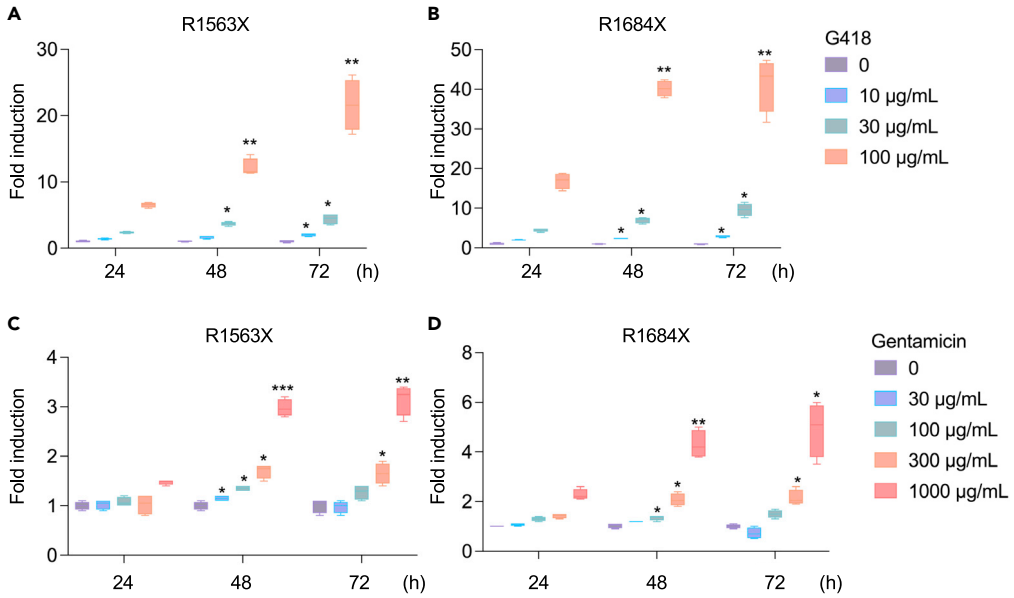

Figure 4. PTC readthrough efficiency is dependent on both dose and treatment time

Cells stably expressing NanoLuc fused to COL4A5-R1563X or R1683X and Luc2 (for normalization) were treated with low-dose G418 (A, B) or gentamicin (C, D) for the indicated times. G418 and gentamicin induced PTC readthrough in the highly susceptible mutants R1563X and R1683X in a dose- and treatment time-dependent manner. The box extends from the 25th to 75th percentiles. Data are represented as mean ± SEM. Statistical analysis was performed using two-way ANOVA with Dunnett's multiple comparisons test (n = 4). *, $p < 0.05$; **, $p < 0.01$; ***, $p < 0.005$ vs. no treatment

(Figure 5G). Only ELX-02 and RTC13 significantly induced PTC readthrough of *COL4A5-G5X* (Figures 5B–5L and S1B). However, the extent of induction was much less than in the case of *COL4A5-R1563X* (Figures 5B and 5H). These results indicate that PTC readthrough was not strongly induced in the G418-non-susceptible *COL4A5-G5X* variant by either ELX-02, which has the same mechanism as G418, or DAP, which exerts its effects via a different mechanism.

Enhancer drugs improve the efficiency of aminoglycoside-induced PTC readthrough

Several PTC readthrough enhancer compounds have been developed to reduce aminoglycoside-induced toxicity by lowering the dose required for sufficient PTC readthrough. The PTC readthrough enhancer CDX5 was identified in a yeast cell-based assay in the presence of the aminoglycoside paromomycin. The effect of CDX5 was also significant in mammalian cells (Baradaran-Heravi et al., 2016). A more recent study showed that the antimalarial drug mefloquine potentiated G418-mediated PTC readthrough in mammalian cells (Ferguson et al., 2019). Here, we investigated whether readthrough enhancers potentiate aminoglycoside-mediated PTC readthrough in the G418-susceptible *COL4A5-R1563X* and non-susceptible *COL4A5-G5X* variants. Mefloquine and CDX5 derivatives potentiated both G418- and gentamicin-mediated PTC readthrough of *COL4A5-R1563X* (Figures 6A and 6B). On the other hand, only mefloquine potentiated both G418 and gentamicin-mediated PTC readthrough of *COL4A5-G5X* (Figures 6C and 6D). Although aminoglycoside-mediated PTC readthrough of *COL4A5-G5X* was enhanced by mefloquine, the induction was weaker than that for *COL4A5-R1563X* without enhancers.

Functionality of the possible PTC readthrough products of G418-susceptible mutants

So far, we have evaluated *COL4A5* nonsense variants in terms of their susceptibility to PTC readthrough, but whether the resulting protein product is functional or not is also important for therapeutic applications. PTC readthrough drugs suppress PTC by facilitating the insertion of near-cognate aminoacyl-tRNAs into the ribosomal-A site during protein translation. Therefore, the readthrough product is often a full-length protein with an incorrect amino acid at the PTC. If such a substitution impairs the function of the protein, it may be difficult to rescue the variant phenotype even if a full-length protein is produced.

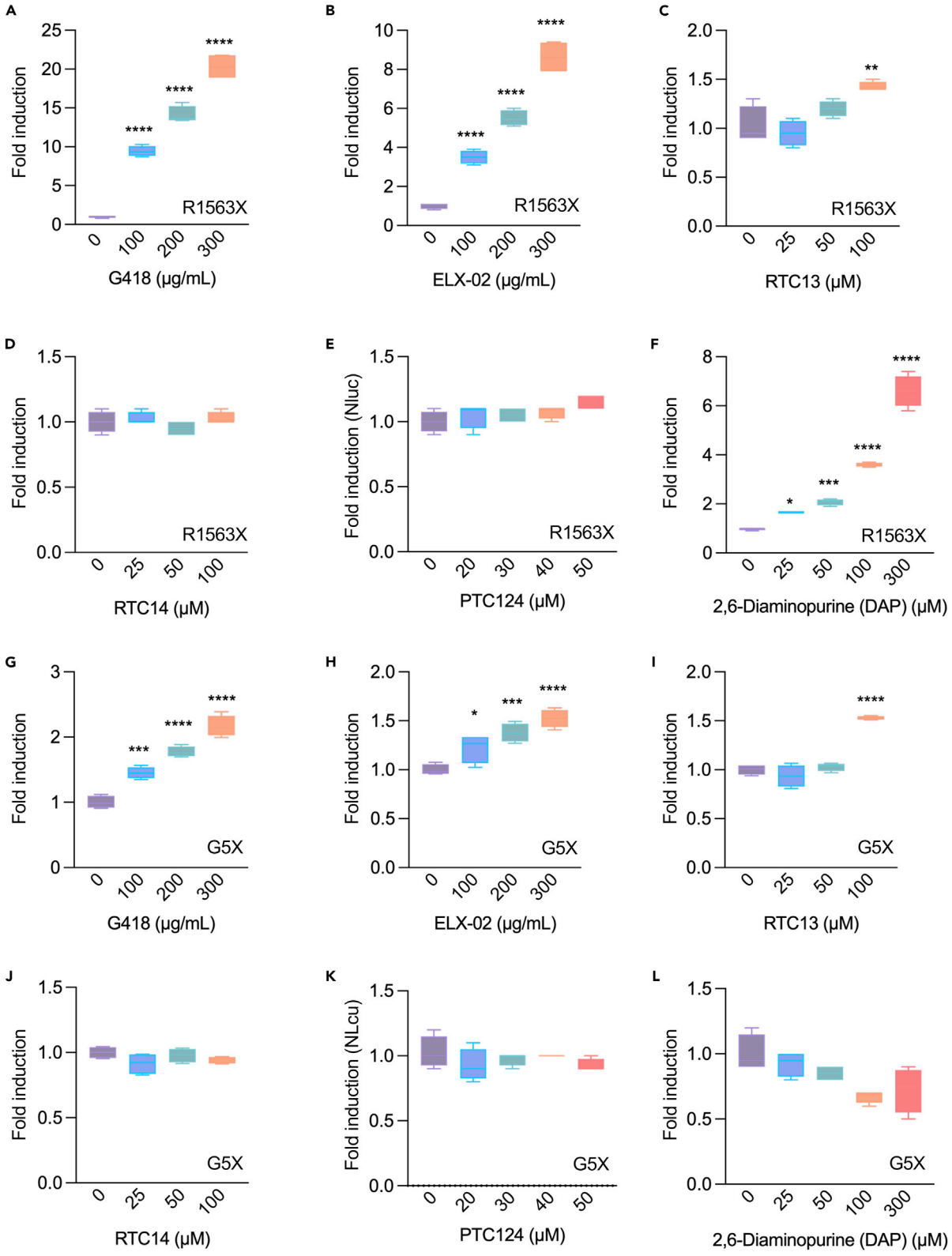
A
Fold induction
R1563X
G418 (μg/mL)
B
Fold induction
R1563X
ELX-02 (μg/mL)
C
Fold induction
R1563X
RTC13 (μM)
D
Fold induction
R1563X
RTC14 (μM)
E
Fold induction (Nluc)
R1563X
PTC124 (μM)
F
Fold induction
R1563X
2,6-Diaminopurine (DAP) (μM)
G
Fold induction
G5X
G418 (μg/mL)
H
Fold induction
G5X
ELX-02 (μg/mL)
I
Fold induction
G5X
RTC13 (μM)
J
Fold induction
G5X
RTC14 (μM)
K
Fold induction (NLcu)
G5X
PTC124 (μM)
L
Fold induction
G5X
2,6-Diaminopurine (DAP) (μM)

Figure 5. Designer aminoglycoside and non-aminoglycoside PTC readthrough drugs induce PTC readthrough of the highly susceptible variant *COL4A5-R1563X*

(A–F) Luminescence was measured in cell lysates from HEK293 cells co-transfected with CMV-NanoLuc-fused COL4A5-R1563X plasmid and HSV-TK-Luc2 (firefly) for normalization. COL4A5-R1563X-NanoLuc-expressing cells were treated with serial dilutions of the indicated drugs. ELX-02, RTC13, and DAP significantly induced PTC readthrough of COL4A5-R1563X. The box extends from the 25th to 75th percentiles. Data are represented as mean ± SEM. (G–L) Luminescence was measured in cell lysates from HEK293 cells co-transfected with CMV-NanoLuc-fused COL4A5-G5X plasmid and HSV-TK-Luc2 (firefly) for normalization. COL4A5-G5X-NanoLuc-expressing cells were treated with serial dilutions of the indicated drugs. ELX-02 and RTC13 significantly induced readthrough of COL4A5-G5X. However, as with the G418-mediated readthrough of COL4A5-G5X, the efficiency was lower than that of COL4A5-R1563X. The box extends from the 25th to 75th percentiles. Data are represented as mean ± SEM. Statistical analysis was performed using one-way ANOVA with Dunnett's multiple comparisons test (n = 4). *, $p < 0.05$; ***, $p < 0.005$ vs. no treatment

To begin to investigate whether the PTC readthrough products from G418-susceptible variants are functional, we utilized a split-NanoLuc-based collagen IV α3α4α5 heterotrimer formation assay. This platform assays α3α4α5 heterotrimer formation by measuring the luminescence produced by the proximity of NanoLuc fragments fused to the ends of COL4A3 and COL4A5 that are brought together during the formation of COL4A3/4/5 heterotrimers (Figure 7A) (Omachi et al., 2018). Most pathogenic *COL4A5* missense variants affect α3α4α5 heterotrimer formation and prevent production of functional collagen IV α3α4α5, which causes Alport syndrome. Therefore, assessing whether PTC readthrough products can assemble into α3α4α5 heterotrimers is important for evaluating the feasibility of PTC readthrough therapy.

It is known that during G418-induced PTC readthrough, Arg, Trp, and Cys are inserted for UGA, Tyr and Gln are inserted for UAA, and Gln is inserted for UAA (Dabrowski et al., 2018). The potential readthrough products from G418-susceptible *COL4A5* variants are shown in Table 1. In several cases, it is possible that PTC readthrough will result in production of some wild-type protein. To investigate the function of the mutant readthrough products, all possible missense mutant substitutions were generated by site-directed mutagenesis and assayed using the C-terminal tagged split NanoLuc-based α3α4α5 heterotrimer assay. The luminescence reflecting heterotrimer formation was significantly decreased intracellularly and extracellularly for some readthrough products from *C1521X*, *R1563X*, *C1567X*, *W1594X*, *R1683X*, and *C1684X*. On the other hand, all readthrough products from *C29X*, *S36X*, *E130X*, *S1632X*, and *K1689X* retained the ability to form α3α4α5 heterotrimers (Figures 7B and 7C). It should be noted that for Arg (R) codons mutated to UGA, more than half of the product is the wild-type R (Roy et al., 2016), so a higher percentage of functional full-length proteins are produced than for Cys (C) to UGA and Trp (W) to UGA mutants. For *C29X*, *S36X*, and *E130X*, the variants are located close to the N-terminus; thus, in addition to the C-terminal tag assays (Figure 7A, left), we also evaluated the function of readthrough products using the N-terminal tag system (Figure 7A, right). The extent of heterotrimer formation for *C29X*-derived products was reduced by half, whereas *S36X*- and *E130X*-derived products retained their functions (Figure 7D). These results indicate that inducing PTC readthrough is a valid approach for a subset of COL4A5 nonsense variants.

Aminoglycosides induced PTC readthrough of *Col4a5-R1563X* in primary kidney cells derived from mutant mice

Although we evaluated PTC readthrough in cell systems overexpressing mutant cDNAs, our ultimate goal is to induce PTC readthrough of nonsense mutant mRNA derived from endogenous *COL4* genes. There are two strains of mouse models for Alport syndrome that carry a *Col4a5* nonsense mutation: the *Col4a5-G5X* mouse (Rheault et al., 2004) and the *Col4a5-R471X* mouse (Hashikami et al., 2019). Our cell-based assay identified G5X as a non-responsive nonsense variant. Furthermore, R471X is not conserved in the human genome (human: Q471X (UAA), mouse R471X (UGA)). Therefore, we generated an Alport syndrome mouse model carrying the *Col4a5-R1563X* nonsense mutation, a variant susceptible to PTC readthrough in cell-based assays (Figures 1A and 2A). We designed a specific single guide (sg) RNA targeting near the codon of interest. Then, the sgRNA, Cas9 protein, and a single-stranded DNA oligonucleotide carrying the mutation were introduced into zygotes by electroporation (Figure 8A) to produce founders. Because the *Col4a5-R1563X* variant is located near an exon-intron junction, we assayed for splicing abnormalities by RT-PCR and Sanger sequencing using RNA from *Col4a5-R1563X* mice. This assay revealed no splicing abnormalities and showed that the targeted mutation was correctly inserted (Figure 8B). The absence of type IV collagen α3α4α5 in the GBM of *Col4a5-R1563X* mice was confirmed by immunofluorescence (Figure 8C).

To directly investigate the feasibility of bypassing an endogenous *Col4a5* nonsense variant by PTC readthrough, we studied primary kidney cells from *Col4a5* nonsense mutant mice. We investigated COL4A5

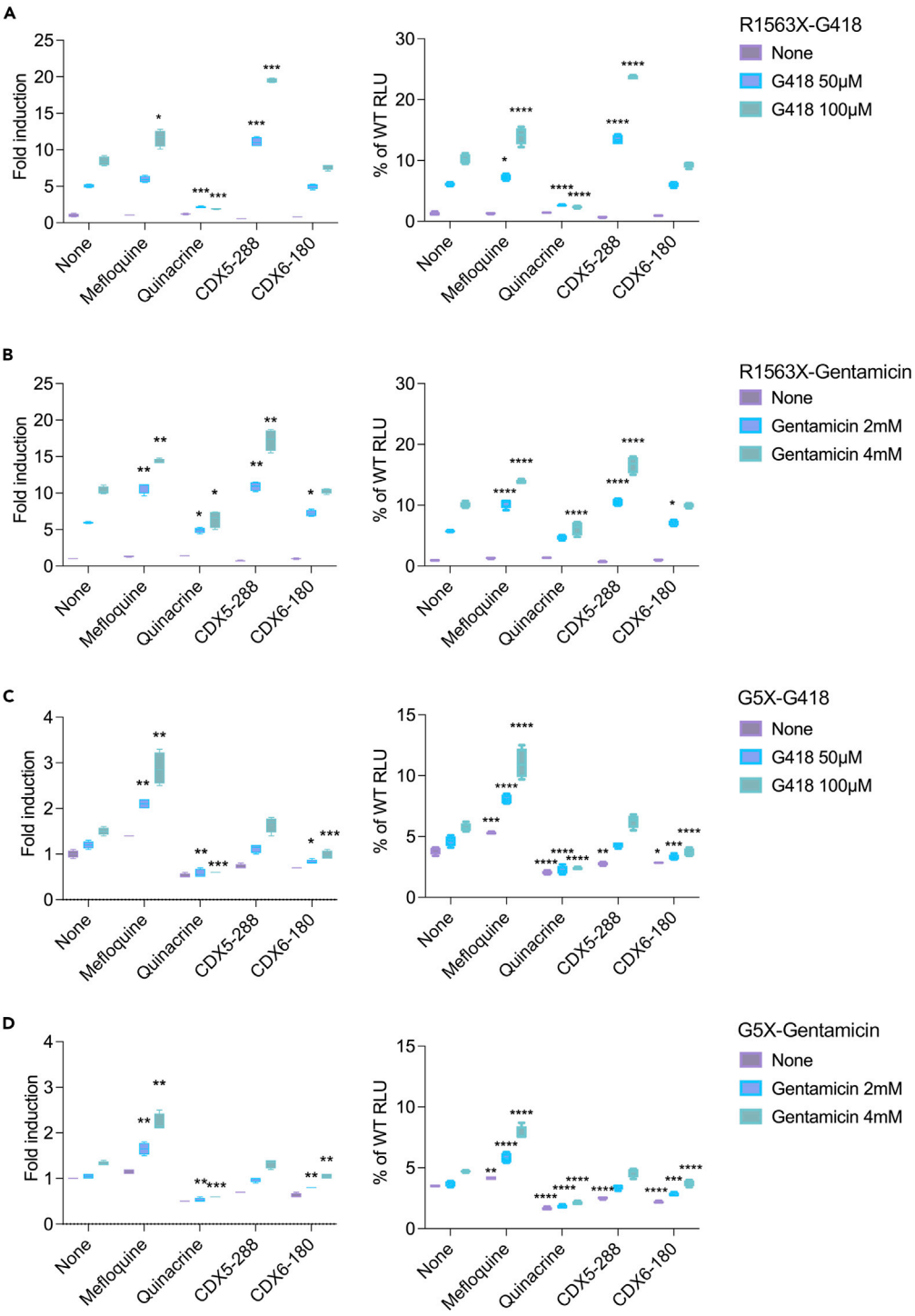

Figure 6. PTC readthrough enhancer drugs increase the efficiency of readthrough

Luminescence was measured in cell lysates from HEK293 cells co-transfected with CMV-NanoLuc-fused COL4A5-R1563X (A, B) or -G5X (C, D) and HSV-TK-Luc2 (firefly) for normalization. Cells were treated with the indicated doses of G418 (A, C) or gentamicin (B, D) supplemented with the indicated readthrough enhancer compounds at 20 μM, and the efficiency of readthrough was compared to WT. Mefloquine and CDX-288 enhanced the readthrough efficacy of both G418 and gentamicin in COL4A5-R1563X-expressing cells. CDX6-180 slightly enhanced gentamicin-mediated PTC readthrough of

Figure 6. *Continued*
COL4A5-R1563X. In contrast to R1563X, only mefloquine enhanced readthrough of COL4A5-G5X. The box extends from the 25th to 75th percentiles. Data are represented as mean ± SEM. Statistical analysis was performed using two-way ANOVA with Dunnett's multiple comparisons test (n = 4). *, $p < 0.05$; **, $p < 0.01$; ***, $p < 0.005$ vs. no G418 or gentamicin treatment

protein expression in primary *Col4a5-R1563X* cells from whole kidney and from isolated glomeruli after treatment with either G418 or gentamicin for 24 h. To increase intracellular protein abundance, the cells were co-treated with the ER-Golgi transport inhibitor Brefeldin A so that COL4A5 protein would accumulate. Full-length COL4A5 protein expression was induced in *Col4a5-R1563X* primary kidney cells and in primary glomerular cells treated with either G418 or gentamicin (Figure 8D). Finally, we compared full-length protein production using primary kidney cultures from mice carrying *Col4a5-R1563X*, which is highly susceptible to PTC readthrough, vs. *-G5X*, which is less susceptible (Figures 1A and 2B). Consistent with our cell-based assays, we found that G418 and gentamicin induced full-length protein synthesis in R1563X cells but not in G5X cells (Figure 8E).

DISCUSSION

The goal of this study was to determine the applicability of PTC readthrough therapy in Alport syndrome caused by nonsense variants. Because the susceptibility to PTC readthrough differs greatly among variants (Bidou et al., 2004; Pranke et al., 2018), the first step would be to determine which variants are susceptible. Because the type IV collagen genes are relatively large with many reported nonsense variants (Crockett et al., 2010; Savige et al., 2016), we thought it is essential to evaluate a simple reporter system with high throughput to cover most of them. In addition, previous studies have shown that PTC readthrough activity is affected by the sequences surrounding the nonsense variants (Stiebler et al., 2014; Wangen and Green, 2020). Therefore, we constructed a reporter using the full-length *COL4A5* cDNA instead of a short cDNA containing the PTC. Because the full-length COL4A5 cDNA itself is about 5 kb, we used NanoLuc as a reporter to construct the fusion gene because of its small size (513 bp) and high sensitivity (England et al., 2016; Hall et al., 2012). The COL4A5-NanoLuc reporter cDNA developed in this study allowed us to identify which of 49 tested *COL4A5* nonsense variants are susceptible to PTC readthrough. Also, this study showed the efficacy of next generation PTC readthrough drugs and potentiator compounds that enhance PTC readthrough activity. Finally, to demonstrate proof of concept for PTC readthrough of an endogenous *Col4a5* nonsense variant, we generated a *Col4a5* mutant mouse line with one of the susceptible nonsense variants, *Col4a5-R1563X*. *Ex vivo* experiments with primary cells showed that aminoglycosides induced PTC readthrough of endogenous *Col4a5-R1563X*.

Through comprehensive variant screening, we found that UGA *COL4A5* nonsense variants were more susceptible to aminoglycoside-mediated PTC readthrough than UAG and UAA. This is consistent with previous studies (Bidou et al., 2004). However, as previously reported, not all UGA PTCs showed high susceptibility (Nudelman et al., 2010), and it was reconfirmed that susceptibility varied depending on the variant. Susceptibility is known to be affected by the surrounding nucleotide sequence. To attempt to determine whether susceptibility is based on the flanking nucleotide sequence, we aligned the cDNA sequences around PTCs that were G418-susceptible and compared them to those flanking the non-susceptible PTCs (Figure S2). However, no overt differences between susceptible and non-susceptible sequences were observed. This suggests that susceptibility is defined by factors other than the peripheral sequence, such as the location of the variant in the gene. Although more detailed comparative studies are needed, these results highlight the importance of screening for PTC readthrough using full-length cDNAs rather than just short cDNA reporters carrying sequence near the PTC.

One limitation of this reporter system is that the presence of nonsense-mediated mRNA decay (NMD) cannot be taken into account because the mRNA derived from the cDNA does not need to be spliced and thus does not have the spliced exon-exon junctions that are required for mRNA surveillance (Popp and Maquat, 2016). mRNAs produced from genes with nonsense variants are partially degraded by NMD (Trcek et al., 2013). Therefore, promotion of basal readthrough by suppression of NMD is one of the therapeutic strategies for nonsense variants, but we have not been able to investigate this. However, because induction of PTC readthrough by NMD inhibition alone is not expected to be very high (Bhuvanagiri et al., 2014), and many aminoglycosides have an activity that inhibits NMD, this limitation is not likely a

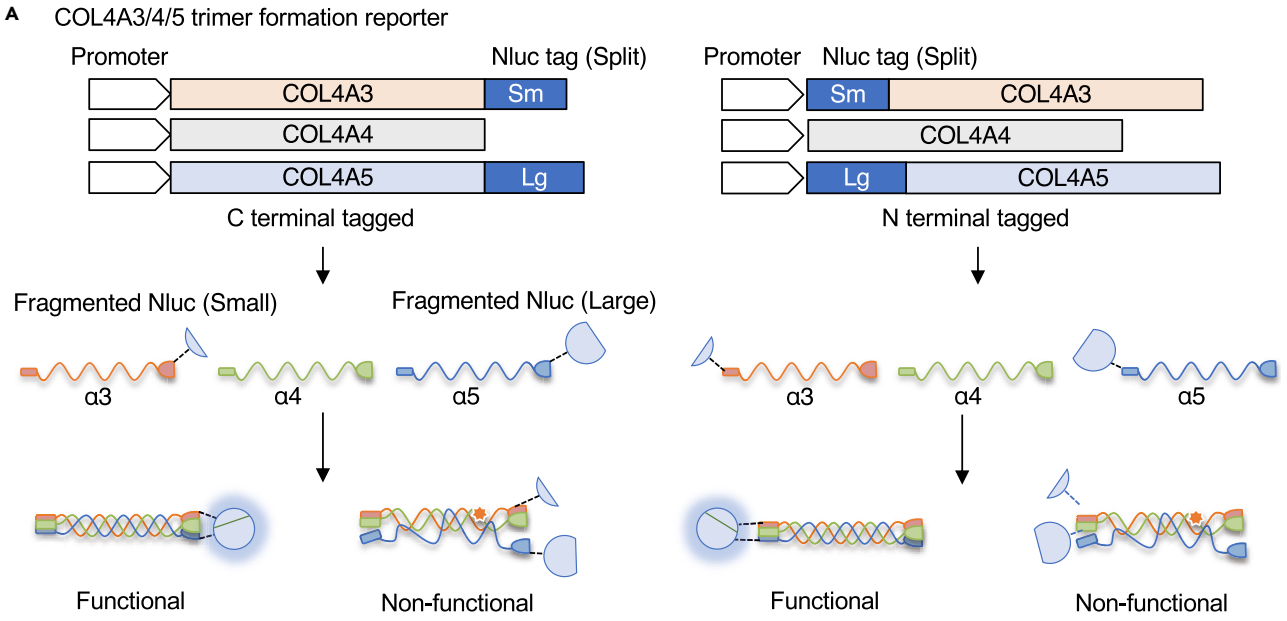
A
COL4A3/4/5 trimer formation reporter
Promoter
Nluc tag (Split)
COL4A3
Sm
COL4A4
COL4A5
Lg
C terminal tagged
N terminal tagged
Fragmented Nluc (Small)
Fragmented Nluc (Large)
α3
α4
α5
Functional
Non-functional

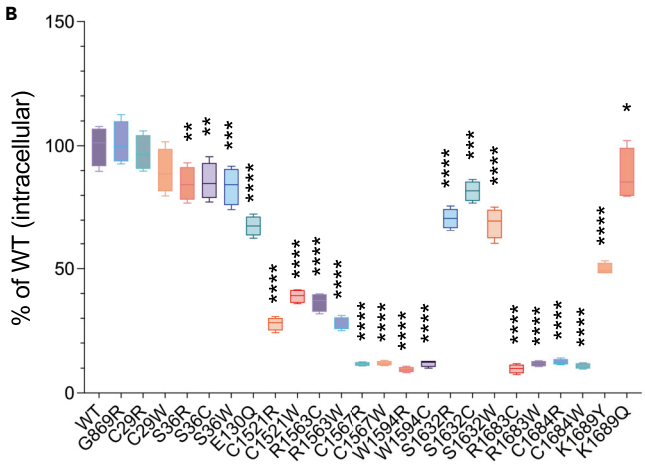
B
% of WT (intracellular)
150
100
50
0
WT
G869R
C29R
C29W
S36R
S36C
S36W
E130Q
C1521R
C1521W
R1563C
R1563W
C1567R
C1567W
W1594R
W1594C
S1632R
S1632C
S1632W
R1683C
R1683W
C1684R
C1684W
K1689Y
K1689Q

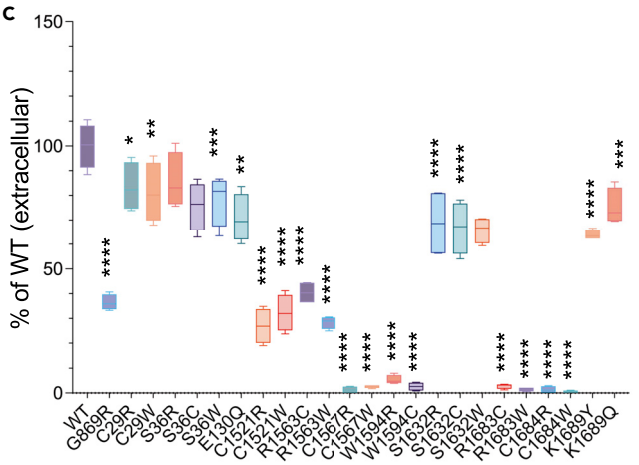
C
% of WT (extracellular)
150
100
50
0
WT
G869R
C29R
C29W
S36R
S36C
S36W
E130Q
C1521R
C1521W
R1563C
R1563W
C1567R
C1567W
W1594R
W1594C
S1632R
S1632C
S1632W
R1683C
R1683W
C1684R
C1684W
K1689Y
K1689Q

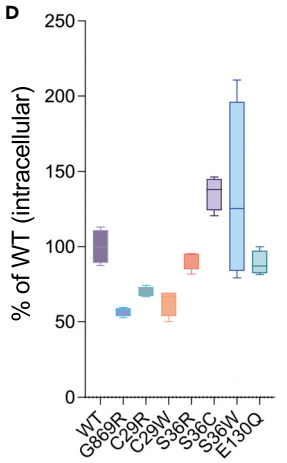
D
% of WT (intracellular)
250
200
150
100
50
0
WT
G869R
C29R
C29W
S36R
S36C
S36W
E130Q

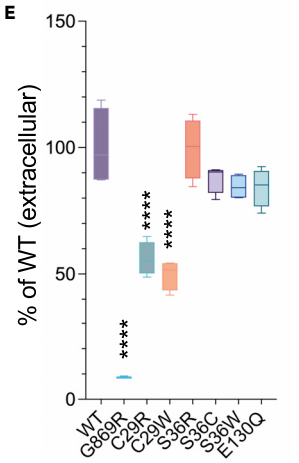
E
% of WT (extracellular)
150
100
50
0
WT
G869R
C29R
C29W
S36R
S36C
S36W
E130Q

Figure 7. Functional analysis of the potential readthrough products from the susceptible COL4A5 variants

(A) Schematic representation of the split NanoLuc-based COL4A3/4/5 trimer formation reporter system. Split NanoLuc fragments (large fragment, Lg; small fragment, Sm) were fused in-frame to the 3′ end of COL4A5 and COL4A3. When COL4A3/4/5 heterotrimers form, split NanoLuc fragments are in close proximity and acquire the ability to produce luminescence. Luminescence was measured in cell lysates (B) and culture media (C) from HEK293T cells expressing C-terminal tagged COL4A5-Lg (WT or the indicated mutants), COL4A3-Sm, and non-tagged COL4A4. HSV-TK-Luc2 (firefly) was included for normalization. In similar studies, luminescence was measured in cell lysates (D) and culture media (E) from HEK293Tcells expressing the analogous N-terminus-tagged proteins. The box extends from the 25th to 75th percentiles. Data are represented as mean ± SEM. Statistical analysis was performed using one-way ANOVA with Dunnett's multiple comparisons test (n = 4). *, $p < 0.05$; **, $p < 0.01$; ***, $p < 0.005$; ****, $p < 0.001$ vs. WT COL4A5

serious problem, but it should be taken into account to accurately determine PTC readthrough activity *in vivo*. To overcome this limitation, CRISPR/Cas9-mediated genome editing could be used to create cells with point mutants in endogenous genes (Anzalone et al., 2020), which would allow the evaluation of PTC readthrough activity under the same conditions as *in vivo*. However, the throughput of this method would be very low, and it is not suitable for evaluating a large number of variants as in the present study.

In addition to defining the readthrough susceptibility of each variant, it is also important to determine whether the possible PTC readthrough products are functional (Brumm et al., 2012). To investigate this, we used split-NanoLuc-based type IV collagen α3α4α5 heterotrimer formation assays to identify which G418-induced full-length but missense variant proteins are functional. Some variants had high readthrough activity but may lose function when a different amino acid from the original is inserted. Many of the variants are located in the COL4A5 C-terminal NC1 domain, which is essential for α5 to form a functional triple-helical structure with other α-chains (Sundaramoorthy et al., 2002). Therefore, structural changes in the protein due to missense variants are likely to interfere with the formation of the correct NC1 complex. However, the results showed that the wild-type S1632 and K1689 residues are not required to form the NC1 complex (Figures 8B and 8C). Also, C29 and S36 in the N-terminal 7S domain and E130 in the N-terminal collagenous domain could be replaced without total inhibition of heterotrimer assembly (Figures 8B–8E). The results suggest that C29 substitution did not impact NC1 complex formation, but partially affected assembly at the N-terminus. This is consistent with the importance of the Cys residue in the 7S domain for disulfide bond formation to other α-chains (Risteli et al., 1980). Using two different assay systems, the PTC readthrough reporter assay and the α3α4α5 heterotrimer assay, we identified several variants that seem truly susceptible to PTC readthrough therapy.

The biggest challenge in PTC readthrough therapy is the toxicity of drugs used at high concentrations for long periods of time to induce synthesis of enough full-length proteins to impact phenotypes. Treatment with high concentrations of aminoglycosides involves the risk of nephrotoxicity and ototoxicity. Fortunately, these issues are being addressed by the development of new PTC readthrough drugs, including new aminoglycoside derivatives (Friesen et al., 2018; Shulman et al., 2014) and non-aminoglycoside compounds (Du et al., 2009; Hamada et al., 2019; Trzaska et al., 2020). Regarding this point, we showed that an aminoglycoside derivative and non-aminoglycoside PTC readthrough drugs induced PTC readthrough in the G418-susceptible *COL4A5-R1563X* variant (Figure 5). In addition, from the viewpoint specific to Alport syndrome, type IV collagen α3α4α5 that incorporates into the GBM should be stable for a long period of time (Liu et al., 2020). This means that once enough type IV collagen α3α4α5 is induced by PTC readthrough and incorporated into the GBM, continuous treatment should not be necessary, though intermittent treatments would likely be required. This suggests that Alport syndrome could be especially suitable for PTC readthrough therapy.

In summary, the present study proposes PTC readthrough as a personalized therapeutic approach for Alport syndrome based on the susceptibility of specific pathogenic nonsense variants to readthrough. Susceptible variants account for about 10% of all nonsense variants, which amounts to <1% of all variants reported in Alport syndrome. Based on the overall frequency of Alport syndrome, the number of patients who could benefit from PTC readthrough therapy is estimated to be 8963 (Table S1). The forms of Alport syndrome caused by nonsense variants, which are classified as truncating variants, are typically more severe than the non-truncating forms, which are usually caused by missense variants. Therefore, the successful development of PTC readthrough therapy would have significant benefits for patients with the most severe forms of Alport syndrome. With various innovations such as the development of designer aminoglycosides and non-aminoglycoside PTC readthrough compounds, PTC readthrough therapy has become an increasingly realistic approach. In fact, some such compounds are in clinical trials for nephropathic cystinosis (ClinicalTrials.gov Identifier: NCT04069260) and cystic fibrosis (ClinicalTrials.gov Identifier: NCT04126473, NCT02139306). The present study provides important information on PTC readthrough-susceptible *COL4A5* variants, and it is hoped

Table 1. Potential PTC readthrough products from G418-susceptible mutants

Nonsense mutation	PTC readthrough products	Predicted ratio (Dabrowski et al., 2018)	Structural location
C29X (UGA)	C29R	64.5 ± 11.8%	7S
	C29C (WT)	17.7 ± 8.0%	
	C29W	17.9 + 6.8%	
S36X (UGA)	S36R	64.5 ± 11.8%	7S
	S36C	17.7 ± 8.0%	
	S36W	17.9 + 6.8%	
E130X (UAA)	E130Y	47.9 ± 14.1%	Collagenous (Gly-X-Y)
	E130Q	52 ± 14.2%	
C1521X (UGA)	C1521R	64.5 ± 11.8%	NC1
	C1521C (WT)	17.7 ± 8.0%	
	C1521W	17.9 + 6.8%	
R1563X (UGA)	R1563R (WT)	64.5 ± 11.8%	NC1
	R1563C	17.7 ± 8.0%	
	R1563W	17.9 + 6.8%	
C1567X (UGA)	C1567R	64.5 ± 11.8%	NC1
	C1567C (WT)	17.7 ± 8.0%	
	C1567W	17.9 + 6.8%	
W1594X (UGA)	W1594R	64.5 ± 11.8%	NC1
	W1594C	17.7 ± 8.0%	
	W1594W (WT)	17.9 + 6.8%	
S1632X (UGA)	S1632R	64.5 ± 11.8%	NC1
	S1632C	17.7 ± 8.0%	
	S1632W	17.9 + 6.8%	
R1683X (UGA)	R1683R (WT)	64.5 ± 11.8%	NC1
	R1683C	17.7 ± 8.0%	
	R1683W	17.9 + 6.8%	
C1684X (UGA)	C1684R	64.5 ± 11.8%	NC1
	C1684C (WT)	17.7 ± 8.0%	
	C1684W	17.9 + 6.8%	
K1689X (UAA)	K1689Y	0.8 ± 7.0%	NC1
	K1689Q	86.5 ± 8.3%	

that new gene-edited mouse models of Alport syndrome carrying the analogous variants in *Col4a5* will facilitate proof-of-concept PTC readthrough studies *in vivo* in the near future.

Limitations of the study

Although we attempted to do so in Table S1, it is difficult to estimate how many patients might actually benefit from PTC readthrough therapy based on the present study alone. G418 induced statistically significant PTC readthrough of 40 of the 49 nonsense variants tested (Figure 2A); 11 were induced > 5-fold, and 17 were induced 2- to 3-fold. These results are from a 24 h treatment, but the actual treatment *in vivo* would be longer term, so the induced protein is expected to accumulate in the GBM over time. In fact, in cell-based assays, prolonging the treatment time by 2–3 days resulted in a significant increase in PTC readthrough product (Figure 4). To determine what percent of variants are amenable to PTC readthrough therapy in a clinically meaningful way, it will be necessary to investigate what level of protein induction is required to produce a therapeutic effect in future studies using mouse models. According to the results of exon skipping therapy in a mouse model of Alport syndrome (Yamamura et al., 2020a), the induction of only a small amount of type IV collagen α3α4α5 in the GBM showed significant therapeutic effects, so

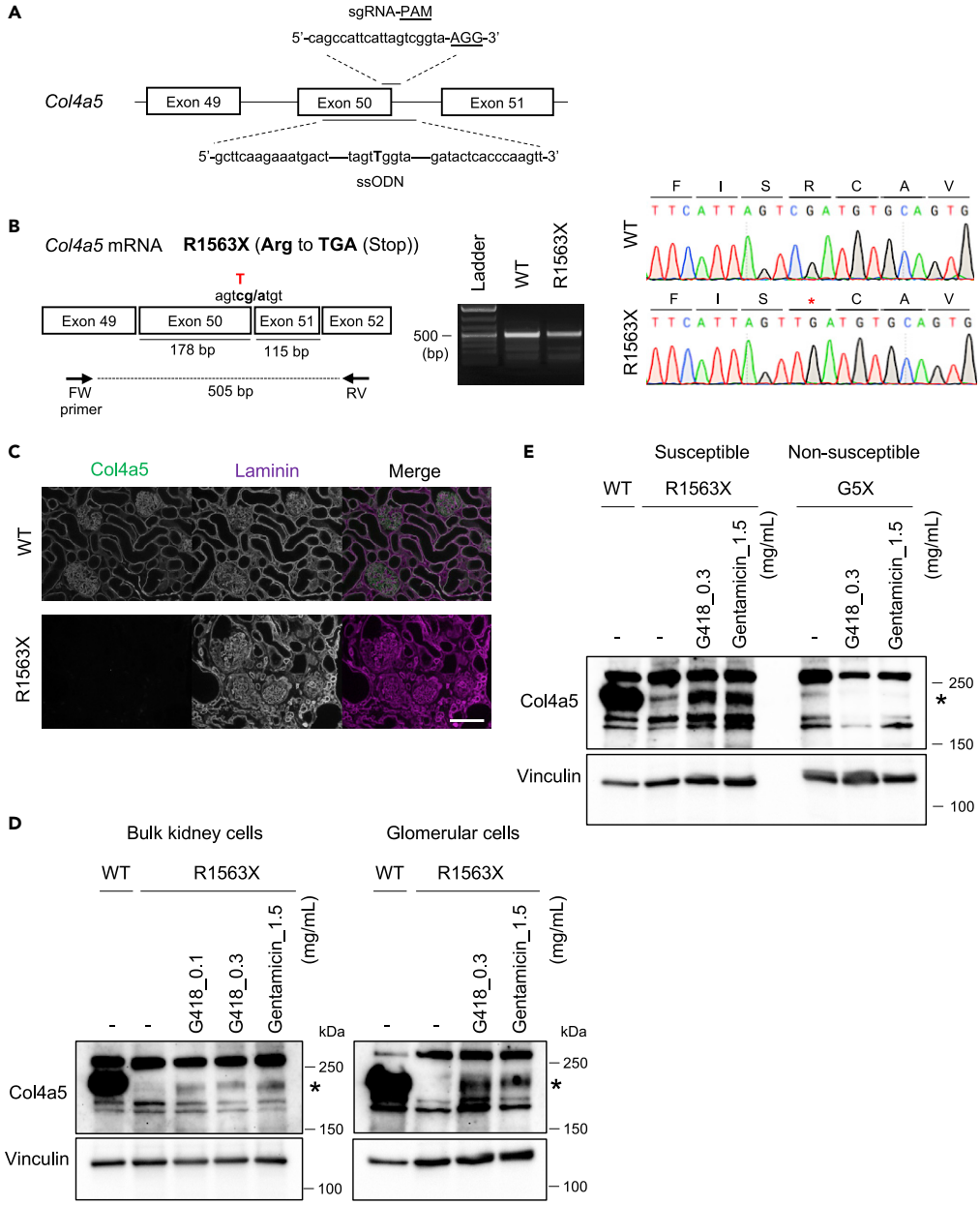

Figure 8. *Ex vivo* experiments with *Col4a5-R1563X* mice shows PTC readthrough of an endogenous nonsense variant

(A) Schematic diagram showing gRNA and ssODN targeting sites to generate the *Col4a5-R1563X* mutant via CRISPR/Cas9.

(B) Schematic diagram shows the R1563X codon (TGA) split between exons 50 and 51. The gel image shows RT-PCR products amplified from exon 49 to 52 from WT and *Col4a5-R1563X* kidney RNA. No splicing abnormalities were detected. Sanger sequencing shows the desired R1563X nonsense mutation.

(C) Immunofluorescence staining for COL4A5 protein shows its absence from *Col4a5-R1563X* mouse kidney. Scale bar: 100 μm.

(D) Immunoblot images of COL4A5 protein shows PTC readthrough of the endogenous *Col4a5-R1563X*. G418 and gentamicin induced full-length protein expression (*) in *Col4a5-R1563X* primary kidney cells (left) and glomerular cells (right).

(E) Comparison of PTC readthrough efficiency between *Col4a5-R1563X* and *-G5X* primary kidney cells. G418 and gentamicin induced PTC readthrough in *R1563X* cells but not in *G5X* cells. This is consistent with cell-based PTC readthrough experiments. Statistical analysis was performed using two-way ANOVA with Dunnett's multiple comparisons test (n = 3). *, $p < 0.05$; **, $p < 0.01$; vs. no G418 or gentamicin treatment

perhaps even low rates of PTC readthrough may, over time, have therapeutic effects. Further studies are clearly necessary before this therapy can be translated into clinical practice, both in terms of readthrough efficiency and toxicity of long-term treatment.

STAR★METHODS

Detailed methods are provided in the online version of this paper and include the following:

- KEY RESOURCES TABLE
- RESOURCE AVAILABILITY
  - Lead contact
  - Materials availability
  - Data and code availability
- EXPERIMENTAL MODEL AND SUBJECT DETAILS
  - Cell culture and cell lines
  - Mouse models
- METHODS DETAILS
  - Chemical compounds
  - Plasmids
  - Transfection, lentivirus production, infection and treatment
  - Cell lysis, gel electrophoresis, and immunoblotting
  - Luciferase assay
  - Immunofluorescence
  - *Ex-vivo* experiments with primary kidney cells
- QUANTIFICATION AND STATISTICAL ANALYSIS

SUPPLEMENTAL INFORMATION

Supplemental information can be found online at https://doi.org/10.1016/j.isci.2022.103891.

ACKNOWLEDGMENTS

This work was supported by grants from the National Institutes of Health (R01DK078314 and R01DK128660 to J.H.M.), the Children's Discovery Institute of Washington University and St. Louis Children's Hospital (MI-II-2019-796 to J.H.M. and CORE-2019-820 to the Pediatric Disease Mouse Models Core), the Japan Society for the Promotion of Science (JSPS) (JP19H03379 to H.K.), the JSPS Program for Advancing Strategic International Networks to Accelerate the Circulation of Talented Researchers (S2803 to H.K.), and the JSPS Program for Postdoctoral Fellowships for Research Abroad (to K.O.). We thank Yoav Segal for the *Col4a5-G5X* mice, David Powell of Chinook Therapeutics for synthesis and validation of ELX-02 and CDX-008, Jennifer Richardson for genotyping, the Genome Engineering and iPSC Center (GEiC) at Washington University for CRISPR reagent validation services, and the Mouse Genetics Core at Washington University for producing gene-edited mice and for mouse husbandry. We also thank the Alport Syndrome Foundation for encouragement to pursue these studies.

AUTHOR CONTRIBUTIONS

K.O. designed the research, conducted experiments, and wrote the manuscript. J.H.M., H.K., and M.R. designed the research and edited the manuscript. All authors discussed the results and provided input on the manuscript.

DECLARATION OF INTERESTS

H.K. holds a patent related to this work, Japanese Patent Application No. 2017-99497. J.H.M. receives research support from Chinook Therapeutics, Lung Therapeutics, Inc., Myonid Therapeutics, and the Alport Syndrome Foundation. The other authors report no conflicts of interest.

Received: July 25, 2021
Revised: December 22, 2021
Accepted: February 4, 2022
Published: March 18, 2022

REFERENCES

Anzalone, A.V., Koblan, L.W., and Liu, D.R. (2020). Genome editing with CRISPR-Cas nucleases, base editors, transposases and prime editors. Nat. Biotechnol. *38*, 824–844. https://doi.org/10.1038/s41587-020-0561-9.

Baradaran-Heravi, A., Balgi, A.D., Zimmerman, C., Choi, K., Shidmoossavee, F.S., Tan, J.S., Bergeaud, C., Krause, A., Flibotte, S., Shimizu, Y., et al. (2016). Novel small molecules potentiate premature termination codon readthrough by aminoglycosides. Nucleic Acids Res. *44*, 6583–6598. https://doi.org/10.1093/nar/gkw638.

Barker, D.F., Hostikka, S.L., Zhou, J., Chow, L.T., Oliphant, A.R., Gerken, S.C., Gregory, M.C., Skolnick, M.H., Atkin, C.L., and Tryggvason, K. (1990). Identification of mutations in the COL4A5 collagen gene in Alport syndrome. Science *248*, 1224–1227. https://doi.org/10.1126/science.2349482.

Bhuvanagiri, M., Lewis, J., Putzker, K., Becker, J.P., Leicht, S., Krijgsveld, J., Batra, R., Turnwald, B., Jovanovic, B., Hauer, C., et al. (2014). 5-azacytidine inhibits nonsense-mediated decay in a MYC-dependent fashion. EMBO Mol. Med. *6*, 1593–1609. https://doi.org/10.15252/emmm.201404461.

Bidou, L., Bugaud, O., Belakhov, V., Baasov, T., and Namy, O. (2017). Characterization of new-generation aminoglycoside promoting premature termination codon readthrough in cancer cells. RNA Biol. *14*, 378–388. https://doi.org/10.1080/15476286.2017.1285480.

Bidou, L., Hatin, I., Perez, N., Allamand, V., Panthier, J.J., and Rousset, J.P. (2004). Premature stop codons involved in muscular dystrophies show a broad spectrum of readthrough efficiencies in response to gentamicin treatment. Gene Ther. *11*, 619–627. https://doi.org/10.1038/sj.gt.3302211.

Brumm, H., Muhlhaus, J., Bolze, F., Scherag, S., Hinney, A., Hebebrand, J., Wiegand, S., Klingenspor, M., Gruters, A., Krude, H., and Biebermann, H. (2012). Rescue of melanocortin 4 receptor (MC4R) nonsense mutations by aminoglycoside-mediated read-through. Obesity (Silver Spring) *20*, 1074–1081. https://doi.org/10.1038/oby.2011.202.

Crawford, D.K., Alroy, I., Sharpe, N., Goddeeris, M.M., and Williams, G. (2020). ELX-02 generates protein via premature stop codon read-through without inducing native stop codon read-through proteins. J. Pharmacol. Exp. Ther. *374*, 264–272. https://doi.org/10.1124/jpet.120.265595.

Crawford, D.K., Mullenders, J., Pott, J., Boj, S.F., Landskroner-Eiger, S., and Goddeeris, M.M. (2021). Targeting G542X CFTR nonsense alleles with ELX-02 restores CFTR function in human-derived intestinal organoids. J. Cyst Fibros. https://doi.org/10.1016/j.jcf.2021.01.009.

Crockett, D.K., Pont-Kingdon, G., Gedge, F., Sumner, K., Seamons, R., and Lyon, E. (2010). The Alport syndrome COL4A5 variant database. Hum. Mutat. *31*, E1652–E1657. https://doi.org/10.1002/humu.21312.

Dabrowski, M., Bukowy-Bieryllo, Z., and Zietkiewicz, E. (2018). Advances in therapeutic use of a drug-stimulated translational readthrough of premature termination codons. Mol. Med. *24*, 25. https://doi.org/10.1186/s10020-018-0024-7.

Du, L., Damoiseaux, R., Nahas, S., Gao, K., Hu, H., Pollard, J.M., Goldstine, J., Jung, M.E., Henning, S.M., Bertoni, C., and Gatti, R.A. (2009). Nonaminoglycoside compounds induce readthrough of nonsense mutations. J. Exp. Med. *206*, 2285–2297. https://doi.org/10.1084/jem.20081940.

Du, M., Keeling, K.M., Fan, L., Liu, X., Kovacs, T., Sorscher, E., and Bedwell, D.M. (2006). Clinical doses of amikacin provide more effective suppression of the human CFTR-G542X stop mutation than gentamicin in a transgenic CF mouse model. J. Mol. Med. (Berl) *84*, 573–582. https://doi.org/10.1007/s00109-006-0045-5.

England, C.G., Ehlerding, E.B., and Cai, W. (2016). NanoLuc: a small luciferase is brightening up the field of bioluminescence. Bioconjug. Chem. *27*, 1175–1187. https://doi.org/10.1021/acs.bioconjchem.6b00112.

Ferguson, M.W., Gerak, C.A.N., Chow, C.C.T., Rastelli, E.J., Elmore, K.E., Stahl, F., Hosseini-Farahabadi, S., Baradaran-Heravi, A., Coltart, D.M., and Roberge, M. (2019). The antimalarial drug mefloquine enhances TP53 premature termination codon readthrough by aminoglycoside G418. PLoS ONE *14*, e0216423. https://doi.org/10.1371/journal.pone.0216423.

Forge, A., and Schacht, J. (2000). Aminoglycoside antibiotics. Audiol. Neurootol. *5*, 3–22. https://doi.org/10.1159/000013861.

Friesen, W.J., Johnson, B., Sierra, J., Zhuo, J., Vazirani, P., Xue, X., Tomizawa, Y., Baiazitov, R., Morrill, C., Ren, H., et al. (2018). The minor gentamicin complex component, X2, is a potent premature stop codon readthrough molecule with therapeutic potential. PLoS One *13*, e0206158. https://doi.org/10.1371/journal.pone.0206158.

Gross, O., Beirowski, B., Koepke, M.L., Kuck, J., Reiner, M., Addicks, K., Smyth, N., Schulze-Lohoff, E., and Weber, M. (2003). Preemptive ramipril therapy delays renal failure and reduces renal fibrosis in COL4A3-knockout mice with Alport syndrome. Kidney Int. *63*, 438–446. https://doi.org/10.1046/j.1523-1755.2003.00779.x.

Gross, O., Tonshoff, B., Weber, L.T., Pape, L., Latta, K., Fehrenbach, H., Lange-Sperandio, B., Zappel, H., Hoyer, P., Staude, H., et al. (2020). A multicenter, randomized, placebo-controlled, double-blind phase 3 trial with open-arm comparison indicates safety and efficacy of nephroprotective therapy with ramipril in children with Alport's syndrome. Kidney Int. *97*, 1275–1286. https://doi.org/10.1016/j.kint.2019.12.015.

Gunwar, S., Ballester, F., Noelken, M.E., Sado, Y., Ninomiya, Y., and Hudson, B.G. (1998). Glomerular basement membrane. Identification of a novel disulfide-cross-linked network of alpha3, alpha4, and alpha5 chains of type IV collagen and its implications for the pathogenesis of Alport syndrome. J. Biol. Chem. *273*, 8767–8775. https://doi.org/10.1074/jbc.273.15.8767.

Hall, M.P., Unch, J., Binkowski, B.F., Valley, M.P., Butler, B.L., Wood, M.G., Otto, P., Zimmerman, K., Vidugiris, G., Machleidt, T., et al. (2012). Engineered luciferase reporter from a deep sea shrimp utilizing a novel imidazopyrazinone substrate. ACS Chem. Biol. *7*, 1848–1857. https://doi.org/10.1021/cb3002478.

Hamada, K., Omura, N., Taguchi, A., Baradaran-Heravi, A., Kotake, M., Arai, M., Takayama, K., Taniguchi, A., Roberge, M., and Hayashi, Y. (2019). New negamycin-based potent readthrough derivative effective against TGA-type nonsense mutations. ACS Med. Chem. Lett. *10*, 1450–1456. https://doi.org/10.1021/acsmedchemlett.9b00273.

Hashikami, K., Asahina, M., Nozu, K., Iijima, K., Nagata, M., and Takeyama, M. (2019). Establishment of X-linked Alport syndrome model mice with a Col4a5 R471X mutation. Biochem. Biophys. Rep. *17*, 81–86. https://doi.org/10.1016/j.bbrep.2018.12.003.

Hudson, B.G., Tryggvason, K., Sundaramoorthy, M., and Neilson, E.G. (2003). Alport's syndrome, Goodpasture's syndrome, and type IV collagen. N. Engl. J. Med. *348*, 2543–2556. https://doi.org/10.1056/NEJMra022296.

Kayali, R., Ku, J.M., Khitrov, G., Jung, M.E., Prikhodko, O., and Bertoni, C. (2012). Read-through compound 13 restores dystrophin expression and improves muscle function in the mdx mouse model for Duchenne muscular dystrophy. Hum. Mol. Genet. *21*, 4007–4020. https://doi.org/10.1093/hmg/dds223.

Lin, X., Suh, J.H., Go, G., and Miner, J.H. (2014). Feasibility of repairing glomerular basement membrane defects in Alport syndrome. J. Am. Soc. Nephrol. *25*, 687–692. https://doi.org/10.1681/ASN.2013070798.

Lincoln, V., Cogan, J., Hou, Y., Hirsch, M., Hao, M., Alexeev, V., De Luca, M., De Rosa, L., Bauer, J.W., Woodley, D.T., and Chen, M. (2018). Gentamicin induces LAMB3 nonsense mutation readthrough and restores functional laminin 332 in junctional epidermolysis bullosa. Proc. Natl. Acad. Sci. U S A *115*, E6536–E6545. https://doi.org/10.1073/pnas.1803154115.

Liu, P., Xie, X., and Jin, J. (2020). Isotopic nitrogen-15 labeling of mice identified long-lived proteins of the renal basement membranes. Sci. Rep. *10*, 5317. https://doi.org/10.1038/s41598-020-62348-6.

Matt, T., Ng, C.L., Lang, K., Sha, S.H., Akbergenov, R., Shcherbakov, D., Meyer, M., Duscha, S., Xie, J., Dubbaka, S.R., et al. (2012). Dissociation of antibacterial activity and aminoglycoside ototoxicity in the 4-monosubstituted 2-deoxystreptamine apramycin. Proc. Natl. Acad. Sci. U S A *109*, 10984–10989. https://doi.org/10.1073/pnas.1204073109.

Miner, J.H. (2011). Organogenesis of the kidney glomerulus: focus on the glomerular basement membrane. Organogenesis *7*, 15275.

Mochizuki, T., Lemmink, H.H., Mariyama, M., Antignac, C., Gubler, M.C., Pirson, Y., Verellen-Dumoulin, C., Chan, B., Schroder, C.H., Smeets, H.J., et al. (1994). Identification of mutations in the alpha 3(IV) and alpha 4(IV) collagen genes in autosomal recessive Alport syndrome. Nat.

Genet. *8*, 77–81. https://doi.org/10.1038/ng0994-77.

Morrison, K.E., Germino, G.G., and Reeders, S.T. (1991a). Use of the polymerase chain reaction to clone and sequence a cDNA encoding the bovine alpha 3 chain of type IV collagen. J. Biol. Chem. *266*, 34–39.

Morrison, K.E., Mariyama, M., Yang-Feng, T.L., and Reeders, S.T. (1991b). Sequence and localization of a partial cDNA encoding the human alpha 3 chain of type IV collagen. Am. J. Hum. Genet. *49*, 545–554.

Nudelman, I., Glikin, D., Smolkin, B., Hainrichson, M., Belakhov, V., and Baasov, T. (2010). Repairing faulty genes by aminoglycosides: development of new derivatives of geneticin (G418) with enhanced suppression of diseases-causing nonsense mutations. Bioorg. Med. Chem. *18*, 3735–3746. https://doi.org/10.1016/j.bmc.2010.03.060.

Omachi, K., Kamura, M., Teramoto, K., Kojima, H., Yokota, T., Kaseda, S., Kuwazuru, J., Fukuda, R., Koyama, K., Matsuyama, S., et al. (2018). A split-luciferase-based trimer formation assay as a high-throughput screening platform for therapeutics in Alport syndrome. Cell Chem Biol. *25*, 634–643 e634. https://doi.org/10.1016/j.chembiol.2018.02.003.

Popp, M.W., and Maquat, L.E. (2016). Leveraging rules of nonsense-mediated mRNA decay for genome engineering and personalized medicine. Cell *165*, 1319–1322. https://doi.org/10.1016/j.cell.2016.05.053.

Pranke, I., Bidou, L., Martin, N., Blanchet, S., Hatton, A., Karri, S., Cornu, D., Costes, B., Chevalier, B., Tondelier, D., et al. (2018). Factors influencing readthrough therapy for frequent cystic fibrosis premature termination codons. ERJ Open Res. *4*. https://doi.org/10.1183/23120541.00080-2017.

Rheault, M.N., Kren, S.M., Thielen, B.K., Mesa, H.A., Crosson, J.T., Thomas, W., Sado, Y., Kashtan, C.E., and Segal, Y. (2004). Mouse model of X-linked Alport syndrome. J. Am. Soc. Nephrol. *15*, 1466–1474.

Risteli, J., Bachinger, H.P., Engel, J., Furthmayr, H., and Timpl, R. (1980). 7-S collagen: characterization of an unusual basement membrane structure. Eur. J. Biochem. *108*, 239–250. https://doi.org/10.1111/j.1432-1033.1980.tb04717.x.

Roy, B., Friesen, W.J., Tomizawa, Y., Leszyk, J.D., Zhuo, J., Johnson, B., Dakka, J., Trotta, C.R., Xue, X., Mutyam, V., et al. (2016). Ataluren stimulates ribosomal selection of near-cognate tRNAs to promote nonsense suppression. Proc. Natl. Acad. Sci. U S A *113*, 12508–12513. https://doi.org/10.1073/pnas.1605336113.

Roy, B., Leszyk, J.D., Mangus, D.A., and Jacobson, A. (2015). Nonsense suppression by near-cognate tRNAs employs alternative base pairing at codon positions 1 and 3. Proc. Natl. Acad. Sci. U S A *112*, 3038–3043. https://doi.org/10.1073/pnas.1424127112.

Savige, J., Storey, H., Il Cheong, H., Gyung Kang, H., Park, E., Hilbert, P., Persikov, A., Torres-Fernandez, C., Ars, E., Torra, R., et al. (2016). X-linked and autosomal recessive Alport syndrome: pathogenic variant features and further genotype-phenotype correlations. PLoS One *11*, e0161802. https://doi.org/10.1371/journal.pone.0161802.

Schiwek, D., Endlich, N., Holzman, L., Holthofer, H., Kriz, W., and Endlich, K. (2004). Stable expression of nephrin and localization to cell-cell contacts in novel murine podocyte cell lines. Kidney Int. *66*, 91–101. https://doi.org/10.1111/j.1523-1755.2004.00711.x.

Shulman, E., Belakhov, V., Wei, G., Kendall, A., Meyron-Holtz, E.G., Ben-Shachar, D., Schacht, J., and Baasov, T. (2014). Designer aminoglycosides that selectively inhibit cytoplasmic rather than mitochondrial ribosomes show decreased ototoxicity: a strategy for the treatment of genetic diseases. J. Biol. Chem. *289*, 2318–2330. https://doi.org/10.1074/jbc.M113.533588.

Stiebler, A.C., Freitag, J., Schink, K.O., Stehlik, T., Tillmann, B.A., Ast, J., and Bolker, M. (2014). Ribosomal readthrough at a short UGA stop codon context triggers dual localization of metabolic enzymes in Fungi and animals. PLoS Genet. *10*, e1004685. https://doi.org/10.1371/journal.pgen.1004685.

Sundaramoorthy, M., Meiyappan, M., Todd, P., and Hudson, B.G. (2002). Crystal structure of NC1 domains. Structural basis for type IV collagen assembly in basement membranes. J. Biol. Chem. *277*, 31142–31153. https://doi.org/10.1074/jbc.M201740200.

Taguchi, A., Hamada, K., Shiozuka, M., Kobayashi, M., Murakami, S., Takayama, K., Taniguchi, A., Usui, T., Matsuda, R., and Hayashi, Y. (2017). Structure-activity relationship study of leucyl-3-epi-deoxynegamycin for potent premature termination codon readthrough. ACS Med. Chem. Lett. *8*, 1060–1065. https://doi.org/10.1021/acsmedchemlett.7b00269.

Taguchi, A., Nishiguchi, S., Shiozuka, M., Nomoto, T., Ina, M., Nojima, S., Matsuda, R., Nonomura, Y., Kiso, Y., Yamazaki, Y., et al. (2012). Negamycin analogue with readthrough-promoting activity as a potential drug candidate for duchenne muscular dystrophy. ACS Med. Chem. Lett. *3*, 118–122. https://doi.org/10.1021/ml200245t.

Trcek, T., Sato, H., Singer, R.H., and Maquat, L.E. (2013). Temporal and spatial characterization of nonsense-mediated mRNA decay. Genes Dev. *27*, 541–551. https://doi.org/10.1101/gad.209635.112.

Trzaska, C., Amand, S., Bailly, C., Leroy, C., Marchand, V., Duvernois-Berthet, E., Saliou, J.M., Benhabiles, H., Werkmeister, E., Chassat, T., et al. (2020). 2,6-Diaminopurine as a highly potent corrector of UGA nonsense mutations. Nat. Commun. *11*, 1509. https://doi.org/10.1038/s41467-020-15140-z.

Wangen, J.R., and Green, R. (2020). Stop codon context influences genome-wide stimulation of termination codon readthrough by aminoglycosides. Elife *9*. https://doi.org/10.7554/eLife.52611.

Wilson, H.M., and Stewart, K.N. (2012). Glomerular epithelial and mesangial cell culture and characterization. Methods Mol. Biol. *806*, 187–201. https://doi.org/10.1007/978-1-61779-367-7_13.

Woodley, D.T., Cogan, J., Hou, Y., Lyu, C., Marinkovich, M.P., Keene, D., and Chen, M. (2017). Gentamicin induces functional type VII collagen in recessive dystrophic epidermolysis bullosa patients. J. Clin. Invest *127*, 3028–3038. https://doi.org/10.1172/JCI92707.

Xue, X., Mutyam, V., Tang, L., Biswas, S., Du, M., Jackson, L.A., Dai, Y., Belakhov, V., Shalev, M., Chen, F., et al. (2014). Synthetic aminoglycosides efficiently suppress cystic fibrosis transmembrane conductance regulator nonsense mutations and are enhanced by ivacaftor. Am. J. Respir. Cell Mol Biol. *50*, 805–816. https://doi.org/10.1165/rcmb.2013-0282OC.

Yamamura, T., Horinouchi, T., Adachi, T., Terakawa, M., Takaoka, Y., Omachi, K., Takasato, M., Takaishi, K., Shoji, T., Onishi, Y., et al. (2020a). Development of an exon skipping therapy for X-linked Alport syndrome with truncating variants in COL4A5. Nat. Commun. *11*, 2777. https://doi.org/10.1038/s41467-020-16605-x.

Yamamura, T., Horinouchi, T., Nagano, C., Omori, T., Sakakibara, N., Aoto, Y., Ishiko, S., Nakanishi, K., Shima, Y., Nagase, H., et al. (2020b). Genotype-phenotype correlations influence the response to angiotensin-targeting drugs in Japanese patients with male X-linked Alport syndrome. Kidney Int. *98*, 1605–1614. https://doi.org/10.1016/j.kint.2020.06.038.

STAR★METHODS

KEY RESOURCES TABLE

REAGENT or RESOURCE	SOURCE	IDENTIFIER
Antibodies		
Rat IgG anti-COL4A5 NC1 monoclonal antibody (clone H52)	Chondrex	Cat# 7077
Rat IgG anti-COL4A5 NC1 monoclonal antibody (clone H53)	Chondrex	Cat# 7078
Mouse IgG1 anti-Vinculin monoclonal antibody (clone 7F9)	Santa Cruz	Cat# sc-73614; RRID:AB_1131294
Rabbit IgG anti-Laminin-111 polyclonal antibody	Sigma-Aldrich	Cat# L9393; RRID:AB_477163
Goat IgG anti-Rat IgG secondary antibody, Alexa 488	Invitrogen	Cat# A-11006; RRID:AB_2534074
Goat IgG anti-Rabbit IgG secondary antibody, Alexa 594	Invitrogen	Cat# A-11012; RRID:AB_141359
Chemicals, peptides, and recombinant proteins		
G418 disulfate solution (50 mg/mL)	Sigma-Aldrich	Cat# G8168
RTC13	Sigma-Aldrich	Cat# SML1725
2,6-Diaminopurine (DAP)	Sigma-Aldrich	Cat# 247847
Brefeldin A	Sigma-Aldrich	Cat# B6542
Gentamicin (50 mg / mL)	Life Technologies	Cat# 15750-060
ELX-02	Sussex Research	N/A
Negamycin analog CDX008	WuXi AppTec	N/A
RTC14	ChemBridge	Cat# 5311257
PTC124	Cayman Chemical	Cat# 16758
Lipofectamine 3000 Transfection Reagent	Invitrogen	Cat# L3000001
FuGENE® 6 Transfection Reagent	Promega	Cat# E2691
X-tremeGENE™ 360 Transfection Reagent	Roche	Cat# XTG360-RO
Critical commercial assays		
Nano-Glo® Dual-Luciferase Reporter Assay System	Promega	Cat# N1620
SuperSignal West Pico Chemiluminescent Substrate	Thermo Scientific	Cat# 34580
Amersham ECL select Western Blotting Detection Reagent	Cytiva	Cat# RPN2235
Pierce BCA Protein Assay Kit	Thermo Scientific	Cat# 23225
Experimental models: Cell lines		
Human: HEK293 cells	ATCC	Cat# CRL-1573; RRID: CVCL_0045
Human: 293T cells	ATCC	Cat# CRL-3216; RRID: CVCL_0063
Human: HeLa cells	ATCC	Cat# CCL-2; RRID: CVCL_0030
Mouse: podocyte cells	Schiwek et al., 2004	N/A
Monkey: COS-7 cells	ATCC	Cat# CRL-1651; RRID: CVCL_0224
Experimental models: Organisms/strains		
Mouse: *Col4a5<tm1Yseg>/<G5X>*	The Jackson Laboratory	Cat# 006183; RRID:MGI:3610502
Mouse: *Col4a5<R1563X>*	This study	N/A
Oligonucleotides		
sgRNA for R1563X production, see STAR Methods	This study	N/A
ssODN for R1563X production, see STAR Methods	This study	N/A
Primers for the site-directed mutagenesis, see Table S1	This study	N/A
Primers for splicing analysis in Col4a5-R1563X mouse, see STAR Methods	This study	N/A
Primers for Sanger sequencing see STAR Methods	This study	N/A

(*Continued on next page*)

Continued

REAGENT or RESOURCE	SOURCE	IDENTIFIER
Recombinant DNA		
pNLF1-C	Promega	Cat# N1361
pGL4.54 [luc2/TK]	Promega	Cat# E5061
pNLF1-C-COL4A5-Nluc: WT	This study	N/A
pNLF1-C-COL4A5-Nluc: G5X	This study	N/A
pNLF1-C-COL4A5-Nluc: C29X	This study	N/A
pNLF1-C-COL4A5-Nluc: Y30X	This study	N/A
pNLF1-C-COL4A5-Nluc: S36X	This study	N/A
pNLF1-C-COL4A5-Nluc: E130X	This study	N/A
pNLF1-C-COL4A5-Nluc: Q182X	This study	N/A
pNLF1-C-COL4A5-Nluc: E228X	This study	N/A
pNLF1-C-COL4A5-Nluc: R226X	This study	N/A
pNLF1-C-COL4A5-Nluc: E287X	This study	N/A
pNLF1-C-COL4A5-Nluc: E291X	This study	N/A
pNLF1-C-COL4A5-Nluc: E305X	This study	N/A
pNLF1-C-COL4A5-Nluc: Y320X	This study	N/A
pNLF1-C-COL4A5-Nluc: R373X	This study	N/A
pNLF1-C-COL4A5-Nluc: Q379X	This study	N/A
pNLF1-C-COL4A5-Nluc: Q407X	This study	N/A
pNLF1-C-COL4A5-Nluc: K408X	This study	N/A
pNLF1-C-COL4A5-Nluc: Q471X	This study	N/A
pNLF1-C-COL4A5-Nluc: Q580X	This study	N/A
pNLF1-C-COL4A5-Nluc: Q700X	This study	N/A
pNLF1-C-COL4A5-Nluc: L755X	This study	N/A
pNLF1-C-COL4A5-Nluc: Q928X	This study	N/A
pNLF1-C-COL4A5-Nluc: Q930X	This study	N/A
pNLF1-C-COL4A5-Nluc: E989X	This study	N/A
pNLF1-C-COL4A5-Nluc: Q1016X	This study	N/A
pNLF1-C-COL4A5-Nluc: Q1052X	This study	N/A
pNLF1-C-COL4A5-Nluc: Q1061X	This study	N/A
pNLF1-C-COL4A5-Nluc: S1071X	This study	N/A
pNLF1-C-COL4A5-Nluc: K1097X	This study	N/A
pNLF1-C-COL4A5-Nluc: Q1180X	This study	N/A
pNLF1-C-COL4A5-Nluc: Q1234X	This study	N/A
pNLF1-C-COL4A5-Nluc: K1320X	This study	N/A
pNLF1-C-COL4A5-Nluc: Q1383X	This study	N/A
pNLF1-C-COL4A5-Nluc: Q1499X	This study	N/A
pNLF1-C-COL4A5-Nluc: Q1501X	This study	N/A
pNLF1-C-COL4A5-Nluc: C1521X	This study	N/A
pNLF1-C-COL4A5-Nluc: Y1543X	This study	N/A
pNLF1-C-COL4A5-Nluc: W1538X	This study	N/A
pNLF1-C-COL4A5-Nluc: R1563X	This study	N/A
pNLF1-C-COL4A5-Nluc: C1567X	This study	N/A
pNLF1-C-COL4A5-Nluc: E1574X	This study	N/A
pNLF1-C-COL4A5-Nluc: W1594X	This study	N/A
pNLF1-C-COL4A5-Nluc: Y1597X	This study	N/A

(*Continued on next page*)

Continued

REAGENT or RESOURCE	SOURCE	IDENTIFIER
pNLF1-C-COL4A5-Nluc: S1632X	This study	N/A
pNLF1-C-COL4A5-Nluc: S1661X	This study	N/A
pNLF1-C-COL4A5-Nluc: R1674X	This study	N/A
pNLF1-C-COL4A5-Nluc: R1683X	This study	N/A
pNLF1-C-COL4A5-Nluc: C1684X	This study	N/A
pNLF1-C-COL4A5-Nluc: Q1685X	This study	N/A
pNLF1-C-COL4A5-Nluc: K1689X	This study	N/A
pLVSIN-Puro Human COL4A5-Nluc: WT	This study	N/A
pLVSIN-Puro Human COL4A5-Nluc: R1563X	This study	N/A
pLVSIN-Puro Human COL4A5-Nluc: R1683X	This study	N/A
pLVSIN-Hygro Luc2	This study	N/A
pFC36K SmBiT TK-Neo Human COL4A3	Omachi et al., 2018	N/A
pLVSIN-Puro Human COL4A4	This study	N/A
pFC34K LgBiT TK-Neo Human COL4A5: WT	Omachi et al., 2018	N/A
pFC34K LgBiT TK-Neo Human COL4A5: G869R	This study	N/A
pFC34K LgBiT TK-Neo Human COL4A5: C29R	This study	N/A
pFC34K LgBiT TK-Neo Human COL4A5: C29W	This study	N/A
pFC34K LgBiT TK-Neo Human COL4A5: S36R	This study	N/A
pFC34K LgBiT TK-Neo Human COL4A5: S36C	This study	N/A
pFC34K LgBiT TK-Neo Human COL4A5: S36W	This study	N/A
pFC34K LgBiT TK-Neo Human COL4A5: E130Q	This study	N/A
pFC34K LgBiT TK-Neo Human COL4A5: C1521R	This study	N/A
pFC34K LgBiT TK-Neo Human COL4A5: C1521W	This study	N/A
pFC34K LgBiT TK-Neo Human COL4A5: R1563C	This study	N/A
pFC34K LgBiT TK-Neo Human COL4A5: R1563W	This study	N/A
pFC34K LgBiT TK-Neo Human COL4A5: C1567R	This study	N/A
pFC34K LgBiT TK-Neo Human COL4A5: C1567W	This study	N/A
pFC34K LgBiT TK-Neo Human COL4A5: W1594R	This study	N/A
pFC34K LgBiT TK-Neo Human COL4A5: W1594C	This study	N/A
pFC34K LgBiT TK-Neo Human COL4A5: S1632R	This study	N/A
pFC34K LgBiT TK-Neo Human COL4A5: S1632C	This study	N/A
pFC34K LgBiT TK-Neo Human COL4A5: S1632W	This study	N/A
pFC34K LgBiT TK-Neo Human COL4A5: R1683C	This study	N/A
pFC34K LgBiT TK-Neo Human COL4A5: R1683W	This study	N/A
pFC34K LgBiT TK-Neo Human COL4A5: C1684R	This study	N/A
pFC34K LgBiT TK-Neo Human COL4A5: C1684W	This study	N/A
pFC34K LgBiT TK-Neo Human COL4A5: K1689Y	This study	N/A
pFC34K LgBiT TK-Neo Human COL4A5: K1689Q	This study	N/A
pFN35K SmBiT TK-Neo Human COL4A3	Omachi et al., 2018	N/A
pFN33K LgBiT TK-Neo Human COL4A5: WT	Omachi et al., 2018	N/A
pFN33K LgBiT TK-Neo Human COL4A5: C29R	This study	N/A
pFN33K LgBiT TK-Neo Human COL4A5: C29W	This study	N/A
pFN33K LgBiT TK-Neo Human COL4A5: S36R	This study	N/A
pFN33K LgBiT TK-Neo Human COL4A5: S36C	This study	N/A
pFN33K LgBiT TK-Neo Human COL4A5: S36W	This study	N/A
pFN33K LgBiT TK-Neo Human COL4A5: E130Q	This study	N/A

(*Continued on next page*)

Continued

REAGENT or RESOURCE	SOURCE	IDENTIFIER
pMD2.G	Addgene	#12259
psPAX2	Addgene	#12260
Software and algorithms		
ImageJ	National Institutes of Health	https://imagej.nih.gov/ij/
GraphPad Prism (version 9)	N/A	https://www.graphpad.com/scientific-software/prism/
Image Lab Software (Version 6.01)	Bio-Rad	https://www.bio-rad.com/en-us/product/image-lab-software?ID=KRE6P5E8Z

RESOURCE AVAILABILITY

Lead contact

Further information and requests for resources and reagents should be directed to the lead contact, Dr. Jeffrey H. Miner (minerj@wustl.edu).

Materials availability

Reagents generated in this study are available from the lead contact under Material Transfer Agreements.

Data and code availability

- This paper does not contain any datasets and codes.
- Any additional information required to reanalyze the data reported in this paper is available from the lead contact upon request.

EXPERIMENTAL MODEL AND SUBJECT DETAILS

Cell culture and cell lines

Human embryonic kidney (HEK) 293 cells (ATCC CRL-1573), 293T cells (ATCC CRL-3216) cells and COS-7 cells (CRL-1651) were maintained at 37 ºC, 5% CO_2 in Dulbecco's Modified Eagle's Medium (DMEM) supplemented with 10% heat inactivated fetal bovine serum and penicillin-streptomycin. HeLa cells (ATCC-CCL-2) were maintained at 37 ºC, 5% CO_2 in Minimum Essential Medium supplemented with 10% heat inactivated fetal bovine serum and penicillin-streptomycin. The mouse podocyte cell line (mPCL) (Schiwek et al., 2004) was maintained at 33 ºC, 5% CO_2 in RPMI-1640 supplemented with 10% heat inactivated fetal bovine serum, penicillin-streptomycin and recombinant interferon-γ (100U / mL). For PTC readthrough experiments, HEK293, HeLa, mPCL and COS-7 cells were used. We did not use 293T cells for PTC readthrough experiments because 293T cells are G418-resistant. For function tests of the potential PTC readthrough products by split NanoLuc assay, 293T cells were used. Cells stably expressing cDNAs were generated by lentivirus infection. Transduced cells were selected by culturing in DMEM with appropriate antibiotics for 2 weeks.

Mouse models

To generate *Col4a5-R1563X* mice, a single guide RNA (5'-CAGCCATTCATTAGTCGGTA-3') targeting the 3' end of *Col4a5* exon 50, a single-stranded DNA oligonucleotide with the *R1563X* mutation (5'-GCTTCAA GAAATGACTATTCTTACTGGCTTTCCACCCCAGAGCCCATGCCAATGAACATGGAACCCCTGAAGGG ACAGAGCATCCAGCCATTCATTAGTTGGTAAGGCACTGGTTTAGCTTTGACATTTACCAATTACCCCTT AGTTTAGCTAGTAAGAAATCAGTGTAAAATGGATAATCCATGATACTCACCCAAGTT-3'), and Cas9 protein were introduced into FVB/NJ zygotes by electroporation. Mutations in the founder mice were analyzed by deep sequencing after genomic amplification with primers (5'–TCGATTCATCATAGGTACGGCTGG CAGCTG-3'; 5'-GTAGCACTTGGTCTAAGCTGGATGCATCCC-3'). The RNA splicing pattern and mRNA sequence were analyzed by RT-PCR with RNA isolated from male *Col4a5*$^{WT/Y}$ and *Col4a5*$^{R1563X/Y}$ kidney tissues. The primer sequences were: sense, 5'- aacagaagcaccacaatgcccacgg-3'; anti-sense, 5' gcatgtccctc gcccatgacattcg-3'. The splicing pattern between Exons 49 and 52 was determined by agarose gel electrophoresis and by Sanger sequencing. FVB/NJ *Col4a5-R1563X* mice were backcrossed to C57BL/6J mice for

at least four generations. *Col4a5-G5X* mutant mice (*Col4a5*^{tm1Yseg}, JAX: 006183) were obtained from Yoav Segal. RT-PCR analysis of kidney RNA showed that this mutation does not impact RNA splicing (Figure S3). All animal experiments conformed to the National Institutes of Health Guide for the Care and Use of Laboratory Animals and were approved by the Washington University Animal Studies Committee.

METHODS DETAILS

Chemical compounds

G418 disulfate solution (50 mg/mL), RTC13, 2,6-diaminopurine, and Brefeldin A were purchased from Sigma-Aldrich (catalog no. G8168, SML1725, 247847 and B6542). Gentamicin (50 mg / mL) was purchased from Gibco, Life Technologies Corporation (catalog no. 15750-060). ELX-02 was synthesized by Sussex Research. The negamycin analog CDX008 (Figure S1) was synthesized by WuXi AppTec. RTC14 was from ChemBridge Corporation (catalog no. 5311257). PTC124 was purchased from Cayman Chemical (catalog no. 16758).

Plasmids

To generate the COL4A5 with C-terminal NanoLuc fusion expression vector, full-length human COL4A5 cDNA was amplified from pEF6-COL4A5-Myc (Omachi et al., 2018), cloned into pNLF1-C [CMV/Hygro] vector (Promega). pLV-BSD COL4A5-LgBiT (C terminal tag), pLV-Hygro COL4A3-SmBiT (C terminal tag), pLV-Puro COL4A4, pFN33K-COL4A5-LgBiT (N terminal tag) and pFN35K-COL4A3-SmBiT (N terminal tag) were used for split NanoLuc luciferase-based COL4A3/4/5 trimer formation assay (Omachi et al., 2018). For all luciferase assays, pGL4.54 [luc2/TK] (Promega) was used as a co-transfected control vector. The variant COL4A5 expression vectors used in this study were generated by site-directed mutagenesis as previously described. Primer sequences are shown in Table S2. The introduced variants were verified by Sanger sequencing.

Transfection, lentivirus production, infection and treatment

HEK293, HeLa and COS-7 cells were transfected with pNLF1-C-COL4A5-Nluc (WT and mutants) and pGL4.54 [luc2/TK] plasmids by FuGENE 6 transfection reagent (Promega). mPCL were transfected with pNLF1-C-COL4A5-Nluc (WT and mutants) and pGL4.54 [luc2/TK] plasmids by X-treamGENE 360 transfection reagent (Roche). Formation of plasmids/FuGENE 6 or X-treamGENE 360 complexes was performed according to the manufacturer's instructions. At 48 h after transfection, cells were treated with DMEM containing G418 or other PTC readthrough drugs.

To produce lentivirus, 293T packaging cells were seeded at 5.5-6.0 × 10^5 cells per wells in DMEM in 6-well tissue culture plates. Seeded cells were incubated at 37 ºC, 5% CO_2 for ~20 h. Culture media were changed to fresh DMEM with 10% heat inactivated fetal bovine serum and transfected with 1 μg of psPAX2 (Addgene: #12260), 100 ng of pMD2.G (Addgene: #12259), and 1 μg of lentivirus transfer vector per well by Lipofectamine 3000 transfection reagent (Invitrogen) according to the manufacturer's instructions. 24 h after transfection, culture media were changed to DMEM supplemented with 30% heat inactivated fetal bovine serum. Lentivirus-containing supernatants were collected after 24 h and filtered with 0.45 μm PVDF or PES membrane syringe filter unit. HEK293 cells or 293T cells were seeded in filtered lentivirus containing media supplemented with 8 μg/mL polybrene (Sigma) and cultured for 24 h, then cells were cultured in DMEM with 10% FBS and the appropriate antibiotics for 2 weeks (Hygromycin; 200-400 μg/mL, Blasticidin: 10 μg/mL, Puromycin 10 μg/mL).

Cell lysis, gel electrophoresis, and immunoblotting

Transfected HEK293 cells were washed twice with ice-cold phosphate buffered 0.9% saline (PBS) and lysed in RIPA buffer (0.05 M Tris-HCl [pH 7.5], 0.15 M NaCl, 1% v/v Nonidet P-40, 1% w/v Na deoxycholate, and 1% protease inhibitor cocktail). The cell lysates were centrifuged at 14,000 g for 15 min at 4°C, and clear supernatants were collected. The protein concentration was determined using a bicinchoninic acid kit (Thermo), and equal amounts of protein lysates were loaded and separated by SDS PAGE, immunoblotted with anti-COL4A5 NC1 antibody (H52, Chondrex) for human COL4A5 cDNA-transfected HEK293 cells, anti-COL4A5 NC1 antibody (H53, Chondrex) for mouse primary cells, and anti-vinculin antibody (7F9, Santa Cruz), and visualized using Super-Signal West Pico Chemiluminescent Substrate (Thermo) and ECL select Western Blotting Detection Reagent (Cytiva).

Luciferase assay

pNLF1-C-COL4A5-NanoLuc and HSV-TK-Luc2 plasmids were transfected into HEK293, HeLa, mPCL and COS-7 cells. After 48 h, cells were fed with culture media containing the test compounds. At 72 h after transfection, Nano-Glo Dual Luciferase Reporter Assay reagent (Promega) was added, and the luciferase activity in the cell lysates was measured using a GloMax Navigator system (Promega). All luciferase assays were conducted in LumiNunc 96-well white plates (Invitrogen). NanoLuc luciferase was normalized by constitutively expressed firefly luciferase.

Immunofluorescence

Kidneys were harvested from anesthetized 1-month-old male *Col4a5*$^{WT/Y}$ and *Col4a5*$^{R1563X/Y}$ mice, and unfixed kidneys were immersed in O.C.T. compound (Tissue-Tek, Sakura Finetek) in a Cryomold (Tissue-Tek, Sakura Finetek) and frozen in liquid nitrogen. Unfixed 7μm frozen sections were blocked with 1% bovine serum albumin/PBS at room temperature for 1 h. Then, sections were incubated with rat IgG anti-COL4A5 antibody (H53, 1/200) and rabbit IgG anti-laminin-111 antibody (Sigma L9393, 1/200) at room temperature for 2 h. Next, sections were washed with PBS three times and incubated with secondary antibodies; Alexa 488-anti-Rat-IgG antibody (1/200) and Alexa 594-anti-Rabbit-IgG antibody (1/200) in PBS containing 1% normal mouse serum at room temperature for 30 min. Sections were washed three times with PBS, mounted, and observed under a fluorescence microscope.

Ex-vivo experiments with primary kidney cells

Kidneys were removed from anesthetized 1-month-old male *Col4a5*$^{WT/Y}$, *Col4a5*$^{G5X/Y}$, *Col4a5*$^{R1563X/Y}$, and female *Col4a5*$^{WT/WT}$, *Col4a5*$^{G5X/G5X}$, and *Col4a5*$^{R1563X/R1563X}$ mice perfused with PBS. The kidneys were minced to 1-2 mm^2 pieces on ice and digested in 1 mg/mL collagenase and 100U/mL DNase I for 30 min at 37°C. After digestion, they were filtered with a 100μm cell strainer and then centrifuged (200 *g*, 5 min). The supernatants were removed, and tissue pellets were dissociated with PBS. They were filtered with a 100μm cell strainer and then centrifuged (200 *g*, 5 min) again. The supernatants were removed and tissue pellets were dissociated with cell culture media. Cell suspensions were seeded onto type I collagen coated tissue culture dishes. Attached cells were maintained at 37°C, 5% CO_2 in RPMI-1640 supplemented with 10% heat inactivated fetal bovine serum and penicillin-streptomycin, insulin, transferrin, and selenium. After 3 days culture, cells were dissociated with 0.25% trypsin/EDTA and filtered with a 30μm cell strainer and then centrifuged (200 *g*, 5 min). Cell pellets were dissociated with culture media and seeded onto type I collagen coated dishes and used for experiments.

Primary glomerular cells were isolated by a mesh sieving method (Wilson and Stewart, 2012). The kidneys were removed and minced into 1-2 mm^2 pieces on ice. The minced kidneys were filtered with 250 μm and 100 μm cell strainers. The filtered tissue suspension was passed through a 75 μm filter, after which the remaining glomeruli on the mesh were isolated. Isolated glomeruli were cultured on type I collagen-coated dishes. Cells were maintained at 37°C, 5% CO_2 in RPMI-1640 supplemented with 10% heat inactivated fetal bovine serum and penicillin-streptomycin, insulin, transferrin, and selenium. After 6 days culture, cells were dissociated with 0.25% trypsin/EDTA and filtered with a 30μm cell strainer and then centrifuged (200 *g*, 5 min). Cell pellets were dissociated with culture media and seeded onto type I collagen coated dishes and used for experiments. Intracellular proteins were extracted with RIPA buffer (0.05 M Tris-HCl [pH 7.5], 0.15 M NaCl, 1% v/v Nonidet P-40, 1% w/v Na deoxycholate, and 1% protease inhibitor cocktail). mRNA was extracted with TRIzol Reagent (Invitrogen) according to the manufacturer's instructions.

QUANTIFICATION AND STATISTICAL ANALYSIS

Statistical parameters are reported in the Fig. Legends. Immunoblot experiments were performed in triplicate using 3 independent transfections. Luciferase assays were performed in quadruplicate using 4 independent cell cultures. The significance of differences between two groups was assessed using Student's unpaired two-tailed t-tests. For three-group comparisons, we used analysis of variance (ANOVA) with Tukey-Kramer post-hoc or Dunnett's tests. Differences with p values of less than 0.05 were considered statistically significant.